To the Graduate Council:

I am submitting herewith a thesis written by Jennie L. Ducker entitled "Prediction of Water Quality from Printed Wiring Board Processes." I have examined the final copy of this thesis for form and content and recommend that it be accepted in partial fulfillment of the requirements for the degree of Master of Science, with a major in Environmental Engineering.

R. Bruce Robinson, Co-Major Professor

Chris D. Cox, Co-Major Professor

We have read this thesis
and recommend its acceptance:

Accepted for the Council:

Associate Vice Chancellor and
Dean of the Graduate School

PREDICTION OF WATER QUALITY FROM PRINTED WIRING BOARD PROCESSES

A Thesis
Presented for the
Master of Science
Degree
The University of Tennessee

Jennie Lou Ducker
May 2000

ACKNOWLEDGEMENTS

I would like to thank my major professors, Dr. Bruce Robinson and Dr. Chris Cox, for their support and guidance in this endeavor, for their confidence in my research abilities, and for providing me this opportunity. Sincere thanks also go to Dr. Bruce Tschantz for serving on my committee, and for providing a critical examination of this thesis.

Funding for this research project was provided by The United States Environmental Protection Agency (EPA) and The University of Tennessee Center for Clean Products and Clean Technologies (CCPCT), for which I am very grateful. Thanks also go to Jack Geibig of the UTCCPCT for providing information and insight on the printed wiring board industry, and to Hadco and Teradyne for providing access to their facilities and information on their processes.

And finally, I would like to thank Sharon Hale for her technical support and willingness to share her time and wealth of laboratory knowledge.

ABSTRACT

The main source of wastewater contamination in the printed wiring board industry is from drag-out of process chemicals during the manufacturing process. Previous drag-out prediction equations are primarily a function of fluid viscosity and board withdrawal rate, and do not account for the many additional variables common in industry. A series of laboratory drag-out experiments were conducted on simulated alkaline cleaner/conditioner and microetch process baths to quantify drag-out volumes for a range of fluid properties and process variables. Results of the experiments compared favorably with published drag-out volumes. The mean drag-out volume for all experiments was around 91 mL/m^2, with literature values ranging from 16 to 203 mL/m^2. The results also indicate that previous predictive equations do not consistently predict drag-out for the range of variables in PWB manufacturing. Predictive equations for the alkaline cleaner/conditioner bath predicted values ranging from about 65 percent below to 40 percent above measured values. Two equations performed very well for the microetch bath, predicting values within 8 percent, but others predicted poorly at 40 to 75 percent below measured values.

A predictive drag-out model was developed by statistical analyses of the experimental data. Dynamic viscosity, surface tension, board withdrawal rate, drip time, board hole density, tilting the board during the drainage period, and the type of board surface were identified as significant variables at a 10 percent level of

significance. Parameters with the greatest impact on drag-out appear to be dynamic viscosity, surface tension, and board hole density. The empirical prediction equation provides a reliable method to predict drag-out as a function of variables relevant to PWB processes. Once the drag-out mass is determined, the wastewater quality can be predicted by applying a mass balance to the overall wet process.

TABLE OF CONTENTS

CHAPTER PAGE

LIST OF TABLES

LIST OF FIGURES

LIST OF ABBREVIATIONS AND SYMBOLS

a	area of sheet
A	first sample collected
A_c	analyte code
AT	anti-tarnish bath
B	second sample collected
BH	board height
BST	board surface type
C	conductivity
$℃$	degrees celsius
Ca	capillary number
cm^2/s	square centimeters per second
cp	centipoise
$dynes/cm$	dynes per centimeter
D	density
D_o	dimensionless thickness (relationship of g to σ forces)
DO	drag-out
DT	drip time
EC	electroless copper bath
f	film thickness
f_{dr}	thickness of film that drains off the sheet
fps	feet per second
F	facility ID number (sample identification)
F_{dr}	function describing a relationship between the independent variables and thickness of a film that drains off a sheet
FB	field blank
g	acceleration of gravity

g/cm^3	grams per cubic centimeter
h	film thickness in drainage stage
h_o	constant film thickness in withdrawal stage
H	height of board
HD	board hole density
I	identifier code
k	unknown constant determined by experiment
K	viscometer constant
l	mean circumference of platinum iridium ring
L	distance plate is moved from the bath,$(U_w \cdot t_w)$
m	unknown exponent determined by experiments
m_s	mass of solution
mg/L	milligrams per liter
mL/m^2	milliliters per square meter
mL/ft^2	milliliters per square foot
m/s	meters per second
mS/cm	millisiemens per centimeter
M	metals
M_B	bottom menisci
M_T	top menisci
ME	microetch bath
MW	makeup water
nm	nanometers
p	poise
ppm	parts per million
P	process tank
Q	flux, or mass flow rate
R	replicate sample
$R1$	first rinse

$R2$	second rinse
S	surface tension
$S\,G.$	specific gravity
SH	shake board at beginning of drainage period, indicator variable
t	time
t_{dr}	drainage time
t_w	withdrawal time
T	temperature
T_0	dimensionless thickness, (relationship of g to μ forces)
TT	tank type
U_w	velocity of withdrawal
UU	process code
V	volume of solution
ΔV	volume of liquid that drains from the sheet
W	weight
WR	withdrawal rate
x	vertical coordinate
μ	dynamic viscosity
ρ	density
ρ_f	density of stainless steel ball
ν	kinematic viscosity
σ	surface tension
$\angle$	board tilt angle during drainage, indicator variable

LIST OF ACRONYMS

AA	Atomic Absorption
CCPCT	Center for Clean Products and Clean Technologies
EPA	Environmental Protection Agency
HDPE	High Density Polyethylene
MHC	Making Holes Conductive
PWB	Printed Wiring Board
QA/QC	Quality Assurance/ Quality Control

CHAPTER I

INTRODUCTION

Background

The printed wiring board is the foundation for the electronics industry. It is the fundamental connection between computer chips, semiconductors, and other electronic components, and can be found in all areas of modern life. Tremendous technological growth over the last several decades has created an increasing global demand for printed wiring board circuitry. Virtually every industrialized or developing country in the world has a need for these products, and as technological innovations continue and new electronic systems are developed, the growth trend will likely continue into the future.

The manufacture of printed wiring boards can have a significant impact on both public health and the environment. Traditional manufacturing methods use significant amounts of water and energy, generate substantial amounts of waste, and use hazardous chemicals that create potential health and environmental risks. To adequately assess these overall impacts, it is necessary to determine the chemical composition of the raw wastewater discharges from the manufacturing processes, as they are a possible major source of environmental contamination if not properly treated.

Printed wiring board manufacturing is primarily a wet chemistry process with multiple rinsing operations. The primary source of contaminants in the wastewater discharge from a plating line is from *drag-out* of the chemical baths and rinsing operations. Drag-out is the industry term used for the amount of liquid, or chemistry, that adheres to the surfaces of the printed wiring board that is *drug-out* from the process tank and subsequently removed in the succeeding rinse tanks.

Many process variables and bath parameters affect drag-out. Previous work has been done to predict the thickness of thin liquid films flowing down stationary flat plates (Denson, 1970; Kushner, 1951a; Gutfinger and Tallmadge, 1965), and limited investigations have been done to predict drag-out film thickness when flat plates are vertically withdrawn from solutions (Kushner, 1951b; Lang and Tallmadge, 1971; Lee and Tallmadge, 1975; Soroka and Tallmadge, 1971; Tallmadge and Gutfinger, 1967; White and Tallmadge, 1965). However, studies specific to liquid parameters and manufacturing conditions expected in the printed wiring board industry are limited.

Statement of the Problem

Previous research has been conducted that evaluated, among other things, environmental impacts from the production of printed wiring boards (EPA, 1998). This research did not adequately evaluate the impacts of chemicals in the wastewater discharges, which is a potentially significant component of the overall impact. Part

of the reason was due to insufficient information on the water quality of the raw wastewater discharges from the plating lines. Since the primary source of pollutants in the raw wastewater is drag-out from the process baths, predicting drag-out for conditions specific to the printed wiring board industry is necessary to estimate the wastewater quality from these industrial discharges.

Objectives of the Study

Theoretical relationships predicting film thickness as a function of fluid viscosity and plate withdrawal rate are available in the literature (Kushner, 1951a; Kushner, 1951b). Additional theoretical relationships are available that predict film thickness as a function of the fluid capillary number (Soroka and Tallmadge, 1971; Tallmadge and Gutfinger, 1967; Tallmadge and Soroka, 1969; Tekić and Duduković, 1982; White and Tallmadge, 1965), which in turn is a function of the fluid surface tension. Much of the previous research relevant to predicting drag-out from the printed wiring boards only considered fluid viscosity and withdrawal speed (Kushner, 1951a; Kushner, 1951b). Therefore, the objectives of this research are to:

- Determine whether surface tension should affect the drag-out volume in printed wiring board manufacturing by a study of the published theoretical and empirical relationships

- Test the validity of the theoretical and empirical relationships found in the literature using data collected through a series of laboratory drag-out experiments and field sampling of actual printed wiring board facilities

- Determine the significance of variables other than fluid properties by statistical analysis, specifically: board tilt, withdrawal rate, hole density, shaking the board at the beginning of the drain period, and the type of board surface.

- Derive a model incorporating theoretical and empirical factors for predicting drag-out as a function of parameters relevant to printed wiring board processes.

Once a reliable method of predicting drag-out is established, a simple mass balance approach can be used to predict the amount (concentration) of contaminants in the plating line raw wastewater.

CHAPTER II

LITERATURE REVIEW

Articles were identified by a computerized database search of appropriate key words. In addition, both a manual and computerized search *of Chemical Abstracts* was done to identify pertinent literature. Other papers were found from references cited in papers, and from a computerized author search of *Web of Science.*

The literature review was done in several phases. The first phase describes a brief overview of the printed wiring board industry, along with the primary source of pollutants in the raw wastewater generated from these processes. The second phase focuses on drag-out theories, theoretical and empirical prediction equations, and a study of published experimental results. This phase summarizes a thorough literature review performed by Robinson, Cox, and Ducker (1999) as part of a final report to the University of Tennessee Center for Clean Products and Clean Technologies and the U.S. Environmental Protection Agency, entitled "Prediction of Water Quality from Printed Wiring Board Processes." The final and most relevant phase of the review investigates the effects of surface tension on drag-out and drainage of flat plates under conditions applicable to the printed wiring board industry.

Overview of Printed Wiring Board Manufacturing Process

The United States currently has approximately 770 to 820 industrial facilities that manufacture printed wiring boards, with most plants located in California, Minnesota, Texas, Illinois, Massachusetts, and Arizona. About 90 percent of the manufacturers are small to medium-sized businesses with annual sales under $10 million, but around seven percent are large companies with annual sales over $20 million (EPA, 1995). The total global market is approximately $21 billion for printed wiring boards, of which U.S. production accounts for more than $5 billion (EPA, 1995).

Printed wiring boards can be categorized by either substrate material or by layer count. The substrates are generally rigid, flexible, or rigid-flex combinations. Glass-reinforced epoxy-resin is typically used for construction of rigid systems, producing a board less than 0.1 inch thick. Although the trend is toward thinner boards, the most common thickness is 0.062 inches (EPA, 1998). Layer counts are the number of circuit layers on the circuit board, and can be categorized as multi-layer, double-sided, and single-sided. A multi-layer board is more complex, and has more than two circuitry layers with at least one layer imbedded in the board substrate. Rigid multi-layer board production is predominant in the U.S. (EPA, 1998).

Multi-layer boards are constructed by bonding alternating layers of insulating and conducting materials containing circuit designs together. Holes are drilled in the

boards to provide connections to both the surface and embedded layers. In a process referred to as *making holes conductive* (MHC), a coating of conductive material is then deposited in the holes so electrolytic copper plating can occur, since the substrate (epoxy-resin and glass) is not conductive. Electroless copper technology has traditionally been used to plate the copper onto the hole barrels (EPA, 1998), thus *making the holes conductive*. The board is then coated with a photoresist material, the circuit image is transferred to the panel, and the panels are electroplated in a copper solution to form electrical conductors on the circuits and in the holes. Finally, the photoresist is removed along with unnecessary copper leaving isolated conductors in the circuit pattern (EPA, 1995). The basic steps necessary to fabricate a rigid, multi-layered printed wiring board are illustrated in Figure 1.

Pollutant Sources in Raw Wastewater

The production processes in the printed circuit board manufacturing industry are similar to those of the electroplating and metal finishing industries, with the major wastestreams being spent solvents, metal-containing wastewater, and sludges. Metals such as silver, gold, copper, tin, and their alloys, to name a few, are utilized on printed circuit boards because of their high conductivity. Their use in connectors and leads keeps power loss to a minimum. Many metal parts must be protected from corrosion by plating with nickel, gold, silver, tin or lead. These metals, which are major hazardous waste components, are introduced into the raw wastewater

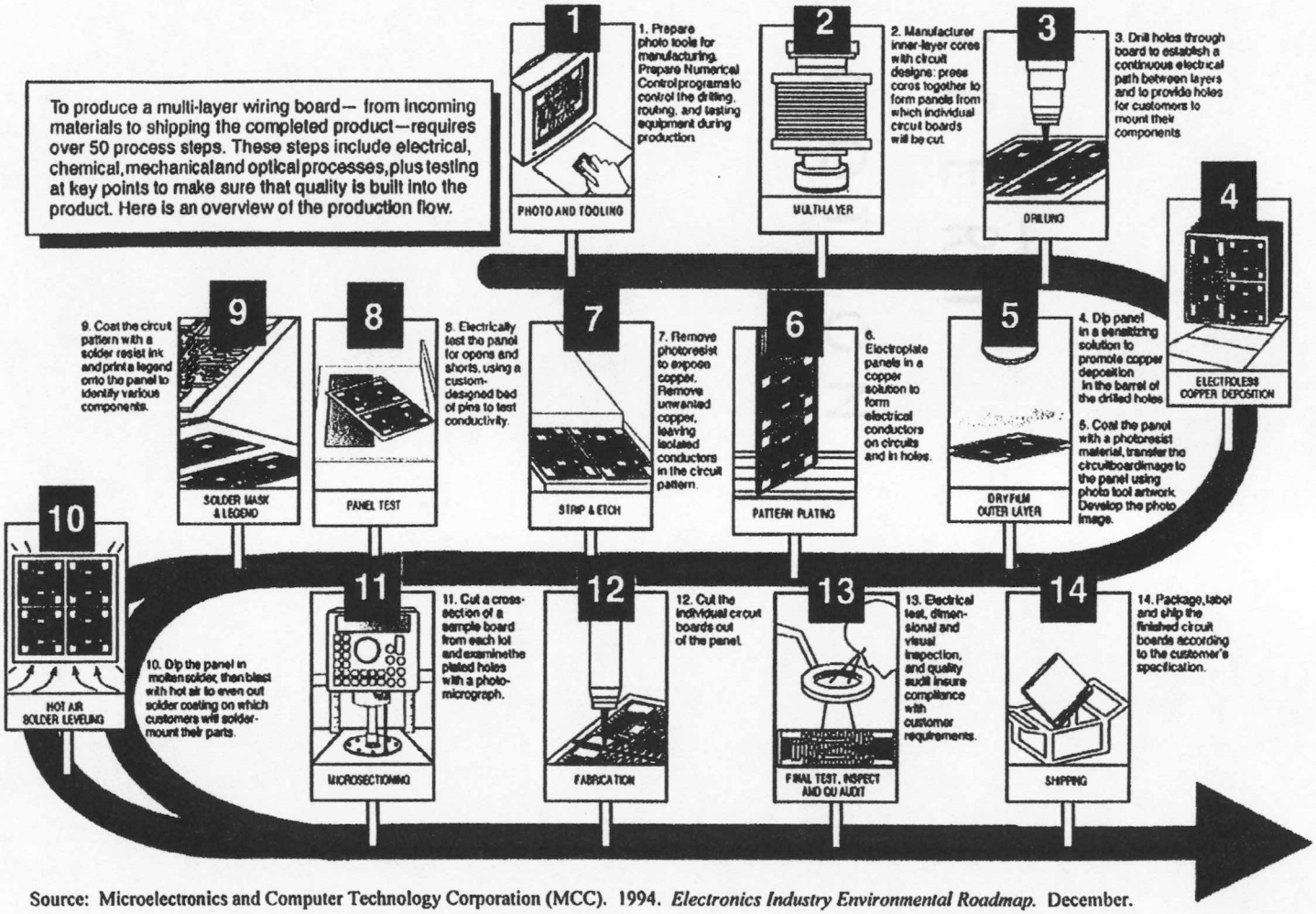

Source: Microelectronics and Computer Technology Corporation (MCC). 1994. *Electronics Industry Environmental Roadmap.* December.

Figure 1. Rigid, Multi-Layer PWB Manufacturing Process Flow Diagram (EPA, 1998)

wastestream (along with other constituents of the process baths) through the disposal of the spent plating baths, waste acids from equipment (rack) cleaning, and used rinse water directly following the plating process (Chang and McCoy, 1990). Another major source of contaminants is the chemical etch (or microetch) processes. Rinses from these processes contain high concentrations of metals, along with dilute levels of the etching solution. Etching baths typically contain sulfuric acid and hydrogen peroxide, ammonium chloride, or ammonium persulfate (Chang and McCoy, 1990). In addition to plating and etching, constituents of other process solutions such as cleaner/conditioner and anti-tarnish baths also contribute to the wastestream in the same manner.

Printed circuit board manufacturing processes are generally operated using vertical, immersion-type, non-conveyorized equipment or horizontal conveyorized equipment. Most facilities in the U.S. use the non-conveyorized vertical immersion system, as conveyorized horizontal equipment is a relatively new innovation, although it is usually more efficient (EPA, 1998).

In the non-conveyorized, immersion-type manufacturing process, several boards (or workpieces) are typically placed vertically in specially designed racks. The racks containing the circuit boards are then immersed in a tank containing the electroplating (or other process) bath where metal deposition (or other process) occurs. The racks are then removed from the process bath and are subjected to

rinsing, typically in a multistage system of rinses. During the course of production, these operations are continuously repeated for subsequent work (Buczko, 1992).

When the racks are withdrawn from the process bath, some of the bath liquid adheres to the surfaces of the circuit boards. These "thin films" of process liquid adhering to the circuit boards are then carried over and subsequently removed in the succeeding rinse tanks. "The volume of solution carried over the edge of a plating or dip tank by an emerging piece of work" is defined as *drag-out* (Kushner, 1951a). The time varying concentration of pollutants in the rinse tank will then depend on the volume of the drag-out, the concentration of the drag-out, the size or volume of the rinse tanks, and the rinse water flow rate (Ledding, 1986). Process rinse water contaminated with drag-out is the largest source of wastewater from most MHC processes, and drag-out losses are estimated to be approximately 95 percent of uncontrolled bath losses (i.e., losses other than from bath replacement, bail-out, and sampling) (Bayes, 1996, as cited by EPA, 1998).

Potential pollutant sources to the raw wastewater other than contamination from process rinses include the disposal of spent bath solutions, waste acids from rack cleaning, and liquid discharges from bath sampling and bail-out. Spent bath solutions are the process baths that can no longer achieve their desired result because of contamination or depletion of necessary constituents. The spent bath solutions are replaced when necessary, and most are disposed of by discharging to the raw

wastewater; however, some etching process baths are sent off-site for processing. Waste acids are produced during equipment cleaning to remove the build-up of metal deposits on the racks. Bath sampling and bail-out includes the disposal of bath solutions after sampling and laboratory analysis, and the removal of bath solution generally done prior to necessary bath additions, respectively.

This study will focus only on drag-out, since it is assumed to be the predominant contributor of pollutants in the raw wastewater. Therefore, it follows that the pollutant mass generation (Kg of pollutant/day, for example) is the mass of pollutants in the drag-out from the process baths. Robinson, Cox and Ducker (1999) found this assumption consistent with the literature, and expressed the relationship as a simple mass balance (Mooney, 1991):

$$\begin{pmatrix} mass\ of\ pollutants \\ in\ drag-out \end{pmatrix} = \begin{pmatrix} mass\ of\ pollutants \\ in\ rinse\ discharge \end{pmatrix} \qquad \text{Equation 1}$$

The volume of waste generation will depend on the rinse water flow rate, since it is the main source of wastewater discharge. The number of rinse tanks for a particular process, the arrangement of the process and rinse tanks, and the rinse water flow rates will affect the concentration and volume of the wastewater discharge, but will not change the total mass of contaminants released.

Drag-out Theories

According to a literature review performed by Robinson, Cox and Ducker (1999), bath fluid properties as well as process variables contribute to the volume of drag-out. Robinson, Cox and Ducker summarized that bath properties influencing the effectiveness of liquid drainage from a circuit board include bath density, surface tension, and viscosity, which is a function of bath temperature and chemistry. Several process variables that potentially reduce drag-out volume include decreasing the withdrawal speed as the circuit board is removed from the process tank, increasing the drainage (drip) period, tilting boards during the drainage period, using drip shields, and using drag-out/drag-in tanks, among others. Robinson, Cox and Ducker concluded that as a result of the complex relationships between the numerous variables and drag-out, estimating drag-out for a series of process baths is a complicated, unsolved problem.

Robinson, Cox and Ducker identified Kushner (1951a) as one of the first researchers to study drag-out in detail. Kushner defined a "withdrawal" stage, in which the board is being withdrawn from the bath but is still in contact with the liquid surface, and a "drainage" stage, in which the board has been completely removed from the liquid, but remains over the tank while liquid drains from the piece. According to Kushner, the thickness of the adhering film is determined by withdrawal; thus, the withdrawal stage is the most important in determining drag-out. Kushner considered the velocity of withdrawal, liquid viscosity and density, along

with surface tension to a minor degree, as factors that control the thickness of the adhering film.

Kushner believed that viscosity is the most important fluid property affecting drag-out. A highly viscous solution will increase the amount of liquid adhering to a board during the withdrawal stage, and decrease the amount of liquid that drains. Robinson, Cox and Ducker further explain in their review of Kushner's work, that some chemicals are surface active, with molecular structures that increase viscosity. This "surface viscosity" may result in more drag-out. Liquid adhering to a board during withdrawal will tend to be less for fluids with higher densities, and drainage will increase. Kushner states, however, that an increase in viscosity usually has more of an effect than the higher density. Robinson, Cox and Ducker cite an example from the literature (Kushner, 1951b) for increasing a sucrose solution concentration from 20 percent to 60 percent. The resulting viscosity increases by 2700 percent, while density increases by only 18 percent.

Although Kushner believed that surface tension was a minor factor, Robinson, Cox and Ducker explained that a lower surface tension will thin the film thickness during withdrawal, increase drainage, and reduce the bead of liquid along the bottom edge of the board. In addition, wetting agents will tend to concentrate in the drag-out, as they are surface active, and therefore be removed at a higher rate than other constituents of the solution. Drag-out will also be reduced by longer

withdrawal and drain times, and Kushner believed that a slower withdrawal velocity was more effective than a longer drainage time. Additionally, Robinson, Cox and Ducker point out that Kushner also recommended orienting the boards to keep drainage distance to a minimum, and tilting the pieces during the drainage period.

Theoretical Drag-out Prediction Equations

Robinson, Cox and Ducker (1999) identified two theoretical drag-out prediction equations from the literature. The first was from Kushner (1951a), and was derived using dimensional analysis:

$$f = 0.02\sqrt{\frac{\mu \cdot H}{\rho \cdot t_w}} \qquad \text{Equation 2}$$

or, simplified:

$$f = 0.02\sqrt{v \cdot U_w} \qquad \text{Equation 3}$$

where:

f = film thickness, cm
μ = dynamic viscosity of electrolyte, g/(cm·s)
H = height of metal sheet
ρ = density of electrolyte, g/cm^3
t_w = withdrawal time, s
v = kinematic viscosity, cm^2/s
U_w = withdrawal rate of metal sheet, cm/s

Robinson, Cox and Ducker point out that Equation 3 is not dimensionally consistent. It was derived using dimensional analysis, but the term for the acceleration of gravity was dropped.

The second equation identified by Robinson, Cox and Ducker was from a paper by Süβ (1992):

$$f = \sqrt{\frac{2v \cdot H \cdot U_w}{9g(H + 4U_w t_{dr})}} \qquad \text{Equation 4}$$

where:

g = gravity, 981 cm/s^2
t_{dr} = drainage time, s

Süβ evaluated both theoretical drag-out prediction equations by conducting experiments to compare the predicted values to measured drag-out volumes. The experiments were performed on 21.0 x 21.4 cm metal sheets with no holes. Sixteen different electrolytes were tested on fluid property ranges as shown in Table 1. Withdrawal speed from the solution was 20 cm/s, and the drainage time was 10 seconds. Robinson, Cox and Ducker reported that neither of the two equations predicted Süβ's measured values very well. The average predicted drag-out and standard deviation for Equation 3 were 96.8 and 17.8 mL/m^2, respectively.

Table 1. Fluid Properties for Drag-out Experiments Conducted by Süβ (1992) (Robinson, Cox and Ducker, 1999)

Fluid Property	*Range*
Concentration	17 – 300 g/L
Density	1.015 – 1.562 g/cm^3
Dynamic viscosity	0.713 – 8.6 cP
Temperature	18 – 59.5°C

Equation 4 had an average predicted drag-out and standard deviation of 15.6 and 2.06 mL/m^2, respectively. The average measured drag-out was 47.4 mL/m^2 with a standard deviation of 16.3 mL/m^2. A linear regression of measured versus predicted drag-out volumes gave an R^2 of 0.021 and 0.012 for Equations 3 and 4, respectively.

According to Robinson, Cox and Ducker, Süβ commented that the equations do not account for liquid that adheres to the board after long drainage periods, which is especially important for rougher surfaces. It was also noted that Süβ's results indicated generally no correlation between drag-out and viscosity. As a result of the poor relationship between predicted versus measured drag-out, Süβ recommended that drag-out estimations be based on measurements instead of calculations.

Empirical Drag-out Prediction Equations

It appears that empirical drag-out prediction equations are even more limited than those based on theory. From a literature review of Robinson, Cox and Ducker (1999), only one empirical relationship was identified, which was derived using dimensional analysis by Kushner (1951a):

$$f = k\left(\frac{U_w \cdot \mu}{\rho \cdot g}\right)^m \qquad \text{Equation 5}$$

where:

k = unknown constant determined by experiments
U_w = velocity of withdrawal, cm/s
m = unknown exponent determined by experiments

According to Robinson, Cox and Ducker, Kushner evaluated Equation 5 based on the experimental work of others, and concluded that the best-fit equation was Equation 3 presented earlier. Equation 3 has also been referenced in other works, such as Pinkerton and Graham's *Electroplating Engineering Handbook* (1984).

Drag-out Prediction Equations Discussion

It should be noted that Equation 3 is applicable only to smooth board surfaces, and does not account for the many small holes common in printed wiring boards. As a result, Robinson, Cox and Ducker point out that the equation would tend to underestimate drag-out for printed wiring boards. Kushner (1951b) argued that Equation 3 predicts drag-out quite nicely for short drainage times, but does not account for liquid that drains off the piece during the drainage period. Therefore, Equation 3 should increasingly overestimate the drag-out for longer drainage times. As an attempt to incorporate the effects of the liquid that drains from the piece, Kushner derived the following relationship:

$$\Delta V = a \cdot f_{dr} = a \cdot F_{dr}(f, \rho, g, \mu, \sigma, t_{dr}) \qquad \text{Equation 6}$$

where:

ΔV = volume of liquid that drains from a rectangular sheet
a = area of sheet
f_{dr} = thickness of the film that drains off the sheet
F_{dr} = function describing a relationship between the independent variables and thickness of film that drains from the sheet
σ = surface tension of the liquid

Therefore, the drag-out volume per unit area at any drainage time, t_{dr}, is:

$$f = 0\ 02\sqrt{v \cdot U_w} - F_{dr}(f, \rho, g, \mu, \sigma, t_{dr}) \qquad \text{Equation 7}$$

No experiments were described in the literature to evaluate Equation 7. However, Robinson, Cox and Ducker point out that Kushner referenced work by Soderberg explaining that drainage times of more than 60 seconds have little effect on reducing drag-out. In addition, McKesson and Wegener (1998) at RD Chemical Company mentions that a long drainage time may result in lower circuit board quality, due to potential chemical drying and tarnishing.

Robinson, Cox and Ducker summarized that predicting the volume of liquid that drains from the board after the board is removed from the liquid is a complex process, for which Kushner could not derive a predictive equation. Although Equation 3 apparently was believed by Kushner to be the best-fit equation for predicting drag-out, Robinson, Cox and Ducker noted that the equation performed poorly when tested by Süβ.

Published Experimental Drag-out Volumes

It should be noted that the prediction equations presented above do not account for the inclination angle of the board during drainage. Robinson, Cox and Ducker reviewed a paper by Süβ (1990) which evaluated methods to minimize drag-out, including the effect of inclination angle during drainage, drainage time, and withdrawal rate. Süβ conducted experiments with chromium plated sheets to determine the effect of drainage time and inclination angle, using concentrations of either 19-20 g/L or 240-250 g/L CrO_3. The results are presented in Table 2. The results show that a 45° inclination angle provided about 33% less drag-out at short drain times, and a horizontal angle had almost 50% less drag-out at long drain times. Increasing drainage time up to around 20 to 30 seconds had a significant effect on reducing drag-out, but longer drainage times had a relatively negligible effect.

Table 2. Effect of Drainage Time and Inclination Angle (Robinson, Cox and Ducker, 1999)

Drainage time, s	*Drag-out, mL/m²*			
	280-320 g/L CrO_3, 0° angle, 40°C	*280-320 g/L CrO_3, 45° angle, 40°C*	*20 g/L CrO_3, 0° angle, 20°C*	*20 g/L CrO_3, 45° angle, 20°C*
0	57	--	64	--
10	28	21	33	24
20	22	13	28	19
30	20	11	25	15
45	19	--	21	13
60	19	10	19	11

The results of Süβ's experiments evaluating the effect of withdrawal rate are presented in Table 3. Süβ found that slower withdrawal rates reduced drag-out. For example, a plate withdrawn at 60 m/min had approximately 25 to 30% more drag-out than a plate withdrawn at 6 m/min. Robinson, Cox and Ducker note that slower withdrawal rates reduce drag-out, but not as much as inclination angle. Robinson, Cox and Ducker also point out that the drag-out volumes reported by Süβ are about half of the volumes reported by other researchers discussed later in this section. Robinson, Cox and Ducker speculated that possible causes could be that Süβ's boards did not contain holes but other studies did; or that Süβ calculated drag-out in terms of the area of both sides of the board, where it appears to be American practice to report drag-out in terms of the area of only one side of the board.

Robinson, Cox and Ducker reviewed the MnTAP/EPA Write Study (Pagel, 1992) at Micom, Inc., which evaluated waste reduction methods from printed wiring

Table 3. Effect of Withdrawal Rate on Drag-out (Robinson, Cox and Ducker, 1999)

Withdrawal rate, m/min	*Drag-out, mL/m²*	
	240-250 g/L CrO_3 (40±1 °C)	*19-20 g/L CrO_3 (20±1 °C)*
3.6	17	21
6	22	26
9	24.5	29
18	26.5	32
36	27	33
60	28	33

board surface finishing processes. Two processes were tested in Micom's MHC line: a micro-etch bath and an electroless copper bath, both with countercurrent rinse tanks following. Micom evaluated two modifications to the processes to see if changes to the way the boards were transferred from the process baths to the rinse tanks could reduce drag-out. The modifications included 1) decreasing the withdrawal rate from the process bath, and 2) using an intermediate withdrawal rate with a longer drain time before moving to the rinse tanks. It should be noted that bath temperatures were not specified in the Micom study. Results of the tests are presented as Tables 4 and 5. Robinson, Cox and Ducker noted that Pagel averaged a broad range of values for the results of drag-out, withdrawal rate, and drain time. The measurements for the baseline and first modification experiments used 136 samples for 12 pairs of racks each. Measurements for the second modification experiments used 109 samples for 9 pairs of racks.

Table 4. Drag-out Test Results on Microetch Bath at Micom, Inc. (Robinson, Cox and Ducker, 1999)

Parameter	*Baseline*	*Slow withdrawal rate*	*Intermediate withdrawal rate & longer drain time*
Drag-out, mL/m^2	129	72.1	76.4
Withdrawal time, s	1.7	14.9	4.3
Withdrawal rate, m/s	0.51	0.056	0.20
Drain time, s	3.4	2.5	12.1
Total time, s	5.1	17.4	16.4
Surface area/rack, m^2	8.2	7.7	8.6
Water flow rate, Lpm	9.8	--	--

Table 5. Drag-out Test Results on Electroless Copper Bath at Micom, Inc. (Robinson, Cox and Ducker, 1999)

Parameter	*Baseline*	*Slow withdrawal rate*	*Intermediate withdrawal rate & longer drain time*
Drag-out, mL/m^2	64.6	32.3	31.4
Withdrawal time, s	1.8	13.9	4.3
Withdrawal rate, m/s	0.48	0.061	0.175
Drain time, s	5.2	3.2	11.9
Total time, s	7.0	17.1	16.3
Surface area/rack, m^2	15.7	15.0	16.3
Water flow rate, Lpm	12.5	--	--

For the microetch bath, Robinson, Cox and Ducker reported a 45% and 41% drag-out reduction for the first and second modifications, respectively. Reductions for the electroless copper bath were 50% and 52% for the first and second modifications, respectively. Robinson Cox and Ducker also noted that reducing drag-out from the microetch bath affects the properties of the bath; therefore, the entire bath may need to be replaced more often due to a build-up of copper in the bath. The case is the opposite for the electroless copper bath; drag-out reduction retains the chemicals in the bath, thus prolonging the bath's useful life.

Robinson, Cox and Ducker's review evaluated several additional references other than those mentioned above to obtain published drag-out volumes (Pinkerton, 1984; Hansan and Zabban, 1959; Yost, 1991; and Chang and McCoy, 1990), in addition to discussions with experts in the surface finishing industry (Sharp, 1998).

Robinson, Cox and Ducker's summary of reported drag-out volumes is presented as Table 6.

Effects of Surface Tension on Drag-out and Drainage

Tallmadge and Gutfinger (1967) studied the entrainment of liquid films on solid surfaces by describing three separate stages of drainage, withdrawal, and removal, as illustrated in Figure 2. In drainage, the liquid flows downward by gravity while the wet support remains stationary in space. Withdrawal is described as the condition where the support is moved with an upward motion from a liquid bath causing entrainment of the liquid onto its surface, while part of the support remains in

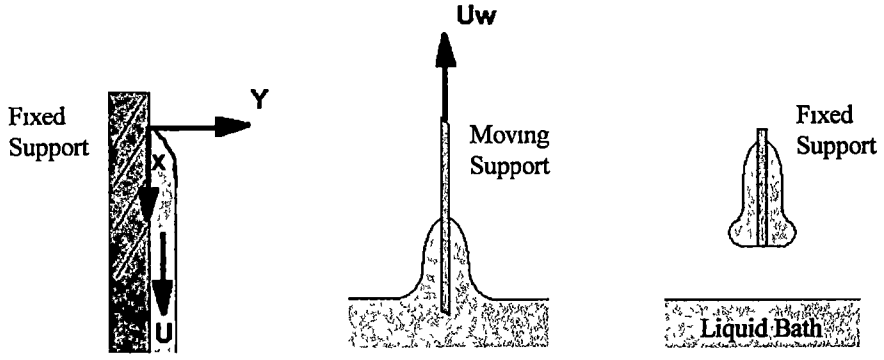

A. Free Drainage B. Unsteady Drainage C. Removal

Figure 2. Drainage, Withdrawal, and Removal (Tallmadge and Gutfinger, 1967)

Table 6. Summary of Reported Drag-out Volumes in the Literature (Robinson, Cox and Ducker, 1999)

Board orientation	*Bath*	*Conditions/description*	*Drag-out, mL/m^2*	*Reference*
Vertical	Micro-etch	Baseline	130	Pagel 1992
"	"	Slow withdrawal rate	72	"
"	"	Intermediate withdrawal rate & longer drain time	76	"
"	Electroless	Baseline	65	"
"	"	Slow withdrawal rate	32	"
"	"	Intermediate withdrawal rate & longer drain time	31	"
Vertical	Not specified	CH_2M-Hill study	103	Sharp 1998
Horizontal	"	Based on experience	27-67	"
Vertical	"	Boards with holes	95	"
"	"	Interlayer boards without holes	41	"
"	"	Vertical parts, well drained	16[1]	Pinkerton 1984
"	"	Vertical parts, poorly drained	82	"
"	"	Vertical parts, very poorly drained	160	"
"	"	Rack plating (used to estimate metals in wastewater for design of wastewater treatment system	203	Hansan & Zabban 1959
Not specified	Not specified	Drag-out value assumed in order to compare costs of rinsing alternatives	162	Yost 1991
"	"	Drag-out value assumed to evaluate waste minimization	160	Chang & McCoy 1990
Vertical	19-20g/L & 240-250 g/L CrO_3	Studies at varying drainage angles, drainage times, and withdrawal rates	12-65	Süβ 1990
Vertical	Various electrolytes	Experimental determinations to test theoretical equations	18-94	Süβ 1992

[1] Suggested by Pinkerton as being the absolute minimum for drag-out on a vertical sheet

contact with the liquid bath. And finally, removal is described as the stage where the support, which is a finite length, is removed from the liquid bath entirely so the entrained film is separated from the surface of the liquid bath.

Since these cases are very complex, Tallmadge and Gutfinger established restrictive conditions for the study. These restrictive conditions are presented as Table 7. The predominant forces in these processes are gravitational, viscous, and interfacial surface tension.

Table 7. Restrictive Conditions for Entrainment of Liquid Films (Tallmadge and Gutfinger, 1967)

Specific Restriction	*Type of Restriction*
1. Wave free and laminar flow	Flow regime
2. Simple axially uniform objects, such as cylinders and flat plates	Solid support geometry
3. Vertical removal	Flow geometry
4. Unobstructed flow	Flow geometry
5. Homogeneous fluid	Liquid material
6. Newtonian fluid	Liquid material
7. Complete wetting and no slip	Surface property
8. No shear at the liquid-gas interface	Surface property
9. Constant temperature	State property
10. Constant pressure	State property

Tallmadge and Gutfinger (1967) further classify drainage as either free or restricted, as shown in Figure 3. Free drainage occurs where the effect of curvature is negligible, and restricted drainage occurs in real cases when effects of curvature can not be neglected; it should be noted that surface tension is one influence on curvature. Free drainage and restricted drainage are closely related; however, restricted drainage is more complex. Figures 3-B and 3-C are examples of restricted, immersed and post-removal drainage, in which surface tension forces have an effect at the top and bottom. Generally in free drainage, curvature is neglected at the top and bottom; therefore, only viscous and gravitational forces are considered.

In problems such as these, the flux, Q, or mass flow rate of the liquid is unknown, but is closely related to the film distribution, entrainment, and the subsequent amount of liquid removed. Tallmadge and Gutfinger (1967) illustrated

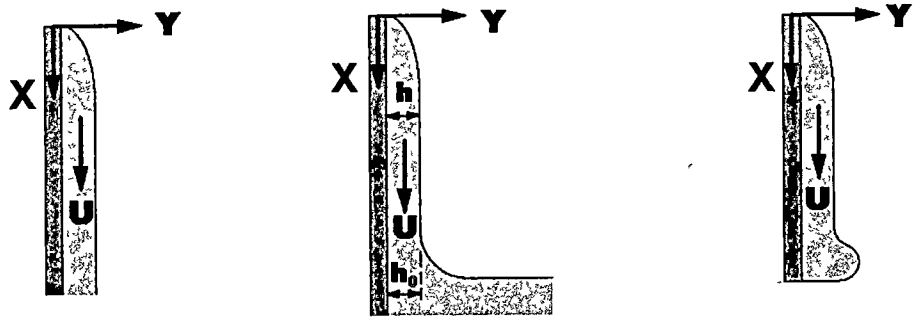

A. Free Drainage

B. Restricted Drainage (Immersed)

C. Restricted Drainage (Post Removal)

Figure 3. Examples of Drainage (Tallmadge and Gutfinger, 1967)

three types of withdrawal in immersed systems, based on differences in the flux. The three types are steady state flux, constant flux, and variable flux. Steady state flux is the condition in which the flux remains constant over time and space, and is described by

$$\frac{\partial Q}{\partial t} = \frac{\partial Q}{\partial x} = 0 \quad for\ all\ x \qquad \text{Equation 8}$$

where:

x = vertical coordinate

Constant flux is the condition in which the flux is constant over a broad range of positions, described by

$$\frac{\partial Q}{\partial t} = \frac{\partial Q}{\partial x} = 0 \quad for\ all\ x_1 << x << x_2 \qquad \text{Equation 9}$$

And the condition when flux varies with both time and position, known as variable flux, can be described as

$$\frac{\partial Q}{\partial t} \neq 0 \qquad \frac{\partial Q}{\partial x} \neq 0 \qquad \text{Equation 10}$$

The three types of withdrawal are illustrated in Figure 4. Unsteady withdrawal of a finite length object is shown in Figure 4-B. Note that the region between the top and bottom menisci (M_T and M_B) illustrates constant flux.

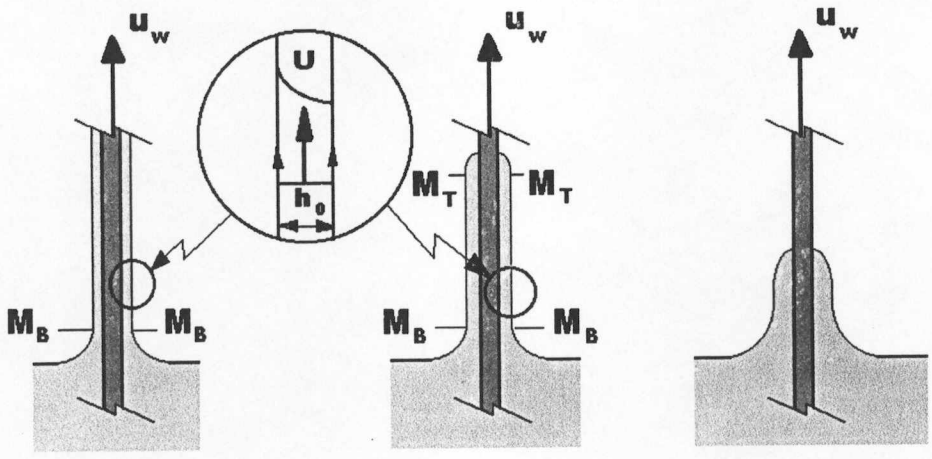

A. Steady State (Continuous)

B. Constant Flux

C. Variable Flux (Unsteady)

Figure 4. Three Types of Withdrawal (Tallmadge and Gutfinger, 1967)

Tallmadge and Gutfinger (1967) divided the film distribution during removal of a flat plat from a liquid bath into five stages, as illustrated in Figure 5. Several flow phenomena occur after the lower end of the object passes through the plane of the liquid surface. The total mass of liquid remaining on the object after separation is termed the removal mass, or drag-out. After separation, the removal mass redistributes, forming a droplet along the bottom of the object that will separate as drippage if the bottom droplet grows large enough. All stages of removal are considered cases of variable flux except for the final film distribution shown in Figure 5, where conditions remain static.

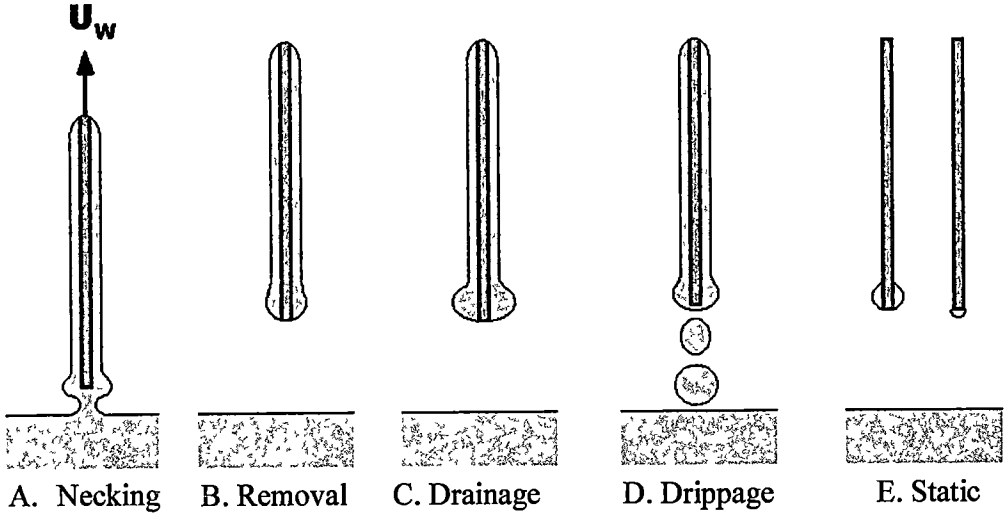

Figure 5. Film Distribution in Removal of Finite Objects (Tallmadge and Gutfinger, 1967)

When the area of constant thickness between the two menisci in Figure 4-B is considered and a negligible change in film thickness with x is assumed, surface tension and inertial forces disappear from the equation, and only viscous and gravity terms remain. Tallmadge and Gutfinger (1967) then applied boundary conditions for flat plates of complete wetting, no slippage, and no shear at the liquid-gas interface, along with an additional boundary condition of a static meniscus. Surface tension and inertial forces were therefore reintroduced, and the gravity-corrected and low speed theories of withdrawal in terms of film thickness were derived.

The gravity-corrected theory arbitrarily divides the film into three regions: 1) the constant thickness region in Figure 4-B, 2) the dynamic meniscus (approaching

M_B from the constant thickness region in Figure 4-B), and 3) the meniscus near the free surface (approaching M_B from the free surface). The theory also includes five assumptions:

1. Curvatures of lower menisci matched (i.e., from the second and third regions above)
2. Negligible viscous term in area near bath surface (static meniscus)
3. One dimensional flow in intermediate, or dynamic meniscus region
4. Negligible effect of flow on interfacial pressure change
5. Negligible film thickness gradient

The gravity corrected theory to predict film thickness, then follows:

$$h_o\left(\frac{\rho g}{\sigma}\right)^{\frac{1}{2}} = 0.944\left(\frac{\mu U_w}{\sigma}\right)^{\frac{2}{3}}\left[1-\frac{h_o^2\rho g}{\mu U_w}\right]^{\frac{2}{3}} \qquad \text{Equation 11}$$

where:

h_o = constant film thickness in withdrawal, cm
σ = surface tension at liquid-gas interface, dynes/cm
U_w = withdrawal velocity, cm/s

According to the literature, the low speed theory of withdrawal was derived from the Landau-Levich theory (Landau and Levich, 1942, as cited by Tallmadge and Gutfinger, 1967), and includes a sixth assumption of a negligible gravitational term:

$$h_0\left(\frac{\rho g}{\sigma}\right)^{\frac{1}{2}} = 0\ 944\left(\frac{\mu U_w}{\sigma}\right)^{\frac{2}{3}} \qquad \text{Equation 12}$$

The gravity corrected theory is cited as the most general, because it reduces to the low speed theory at low withdrawal velocities, when the "capillary number" approaches zero.

Capillary Number

For constant flux withdrawal, film thickness is a function of the withdrawal speed. Tallmadge and Gutfinger (1967) explains that the independent variable, withdrawal speed, is converted into a dimensionless form using fluid properties, and termed the capillary number, *Ca*:

$$Ca = \frac{viscous\ force}{surface\ tension} = \frac{\mu U_w}{\sigma} \qquad \text{Equation 13}$$

More simply stated, the capillary number is a dimensionless velocity term that can be used to correlate data for a range of liquids with a variety of viscosities and surface tensions. According to Tallmadge and Gutfinger, when the capillary number is less than one, surface tension forces tend to predominate. When the capillary number approaches one, viscous forces become much more important and surface tension effects become small. The literature states that the applicability of the capillary number was shown theoretically as far back as 1942 (Landau and Levich, 1942, as cited by Tallmadge and Gutfinger, 1967), and was used independently in empirical correlations for flat plates in 1946 (Blok, 1951, as cited by Tallmadge and Gutfinger, 1967)

Drag-out Prediction Equations That Include Capillary Number

Tallmadge and Gutfinger points out that the Landau-Levich theory (low speed) implied that $U = U_w$ throughout the constant thickness region, and therefore may be called the plug flow theory. In addition, it implies that $h = h_o$. The literature also states that flow thickness-film thickness relationships frequently appear in *"T"* form, therefore, the theoretical prediction of flow thickness for the plug flow equation becomes:

$$T_0 = 0.944 Ca^{\frac{1}{6}} \qquad \text{Equation 14}$$

where:

T_0 = dimensionless thickness

When the capillary number is much less than one (as would be expected for process baths in the printed circuit board industry, due to their ranges of dynamic viscosity, withdrawal rate, and surface tension), surface tension predominates, and entrainment follows the plug flow equation (Equation 14) (Tallmadge and Gutfinger, 1967). To clarify the derivation of Equation 14, it should be noted that the ratio of gravitational force to surface tension is typically expressed as:

$$D_o = h_o \left(\frac{\rho g}{\sigma} \right)^{\frac{1}{2}} \qquad \text{Equation 15}$$

where:

D_o = dimensionless thickness, in ratio of g to σ

The relationship between gravitational and viscous forces is typically expressed as:

$$T_o = h_o\left(\frac{\rho g}{\mu U_w}\right)^{\frac{1}{2}}$$ Equation 16

And the interrelationship between T_o and D_o is:

$$D_o = T_o Ca^{\frac{1}{2}}$$ Equation 17

It should also be noted that Equation 14 does not account for drippage. According to Tallmadge and Gutfinger (1967), the influential parameters are not well understood, and there are no general theories or predictive equations for removal, separation and drippage, although it has been observed and accounted for in numerous experiments.

In a subsequent work, Lang and Tallmadge (1971) termed the removal stage as *postwithdrawal drainage*. To further clarify, postwithdrawal drainage occurs when a flat plate is withdrawn at a constant speed (U_w) for a distance L and then stopped, as illustrated in Figure 6. The resultant film then drains under the influence of gravity, and the location of the liquid-solid-gas junction remains fixed with respect to the solid support. Lang and Tallmadge derived an expression that describes the influence of withdrawal variables on the thickness of postwithdrawal drainage, and separates the process into two parts; the first-stage of withdrawal is used as a boundary condition (or initial profile) for the second stage of drainage. Thus, the postwithdrawal theory of drainage:

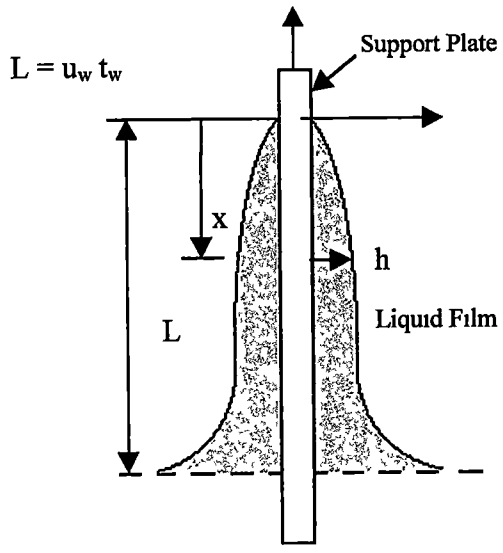

Figure 6. Postwithdrawal Drainage (Lang and Tallmadge, 1971)

$$h = \left[\frac{\mu U_w x}{\rho g (L + u_w t_{dr})} \right]^{\frac{1}{2}} \qquad \text{Equation 18}$$

where:

t_{dr} = drainage time
t_w = withdrawal time
L = distance plate is moved from the bath

Lang and Tallmadge (1971) also explain that since withdrawal time t_w = L/U_w, Equation 18 may be written in the form:

$$h = \left[\frac{\mu x}{\rho g (t_w + tdr)} \right]^{\frac{1}{2}}$$ Equation 19

or

$$\frac{h}{\sqrt{x}} = \left(\frac{\mu / \rho g}{t_w + t_{dr}} \right)^{\frac{1}{2}}$$ Equation 20

It should be noted that although Lang and Tallmadge considered the capillary number in tests, it is not a variable in Equation 20, and therefore, Equation 20 is not a function of surface tension. Lang and Tallmadge tested Equation 20 using a viscous oil over a range of withdrawal speeds (0.2 – 2.2 cm/s), withdrawal times (7 – 80 sec), and distance to top (1 – 4 cm); and the equation performed very well. The capillary numbers tested, however, varied from about 0.1 to 1, so the authors did not expect to see large capillary effects. Lang and Tallmadge believed that at low capillary numbers (i.e., as expected in plating baths), entrainment would be substantially less than that predicted by the viscogravity expressions. They state that some deviation from Equation 20 might occur if lower speeds or lower viscosities were used.

Tekić and Duduković (1982) derived an expression for the prediction of film thickness on a vertical flat plat, based on the concepts of Lang and Tallmadge (1971). Tekić and Duduković determined that the process of postwithdrawal drainage could be split into two phases, with the results of the first stage (withdrawal) used as the

boundary condition for the second stage of drainage. Tekić and Duduković predicted film thickness for the withdrawal stage from the following relationship:

$$T_0 = 0.944 \cdot Ca^{2/3} \qquad \text{Equation 21}$$

When withdrawal is stopped, the resulting dimensionless film thickness derived from Equation 21 is converted to a dimension form, h_0 (using Equation 16), and is then used to predict film thickness during drainage, with the following relationship:

$$h(x,t) = \left[\frac{x}{\frac{\rho g}{\mu} t + h_0^{-2} x} \right]^{1/2} \qquad \text{Equation 22}$$

where:

h = film thickness in drainage stage, cm

Although Tekić and Duduković provide a method to calculate drag-out as a function of surface tension, the derivation of Equation 22 could not be clearly supported and validated in the literature. Therefore, the method was not considered.

It should also be noted that the above relationships, even combined, do not account for separation and drippage; nor do they account for drilled boards, as is common in the printed wiring board industry.

CHAPTER III

METHODS AND MATERIALS

Experimental Approach

The objective of the laboratory study and field sampling had several purposes:

1) to determine if surface tension is a variable that contributes significantly to drag-out in printed wiring board manufacturing,
2) to test theoretical and empirical drag-out relationships from the literature,
3) to determine the significance of process variables on drag-out, and
4) to derive a statistical model incorporating theoretical and empirical factors for drag-out prediction as a function of parameters relevant to printed wiring board processes.

The experimental approach was to conduct laboratory tests for a range of conditions to develop a database that could be used to test and develop drag-out models, and then verify the models by sampling and analysis of process baths and rinses from actual manufacturing processes.

Laboratory Drag-out Volume Study

The procedure for the laboratory drag-out experiments was to simulate two process baths in the manufacturing process of a printed circuit board. A heated chemical bath was set up in the laboratory, and an actual circuit board was utilized to reproduce the variable operating conditions frequently encountered in industry. The volume of liquid that adhered to the circuit board under the variable conditions is the drag-out that, in industry is removed in the succeeding rinse tank(s) and ends up in the wastewater. In the laboratory study, the drag-out volume was gravimetrically measured by placing the wetted circuit board into a plastic bag (instead of a rinse tank) and weighing the plastic bag, circuit board, and drag-out liquid. By knowing the dry weight of the circuit board and plastic bag, and the specific gravity of the liquid, the volume of drag-out was calculated.

Laboratory Drag-out Experiments

Experiments with two types of baths were conducted: a simulated alkaline cleaner/conditioner bath, and a simulated microetch bath. The matrix of experimental conditions that were tested is presented as Table 8.

Apparatus

- 4" x 24" x 30" high density polyethylene (HDPE) tank, supported and stabilized to prevent tipping
- Magna-Whirl Constant Temperature Water Bath, Model MW-1140A-1

Table 8. Experimental Matrix for Laboratory Study of Drag-out Volumes

Experimental conditions	*Drilled board*	*Undrilled board*	*Drilled, etched board*
0.076 m/s (0.25 fps) withdrawal 45° drain angle 10 sec drip time no shaking	•	•	•
0.076 m/s (0.25 fps) withdrawal lengthwise orientation 10 sec drip time no shaking	•		
0.076 m/s (0.25 fps) withdrawal widthwise orientation 10 sec drip time no shaking	•		
0.076 m/s (0.25 fps) withdrawal 45° drain angle 20 sec drip time no shaking	•		
0.076 m/s (0.25 fps) withdrawal 45° drain angle 30 sec drip time no shaking	•		
0.305 m/s (1.0 fps) withdrawal 45° drain angle 10 sec drip time no shaking	•		
0.076 m/s (0.25 fps) withdrawal 45° drain angle 10 sec drip time shake board	•		

- Pump, ITT Jabsco Self-Priming, Model 12290-0001, 115 volt, 3.3 amp, with thermal overload protection
- 20 ft. of ½" diameter stainless steel tubing, coiled to fit inside bottom of HDPE tank
- ½" I.D. Nalgene tubing, lab/food grade, with connection clamps
- 48 liters bath chemistry (Alkaline Cleaner/Conditioner or Microetch)
- Mettler Toledo Electronic Analytical Balance, Model PR5002, Maximum 5100 grams, with cardboard air current shield
- 18" x 24" circuit boards (copper clad with holes; copper clad without holes; etched, with holes)
- Plastic bags, 0.50 mil, 2'6" x 3', 30 gal. capacity
- Whittner Taktell Super-Mini Metronom, Model 886051, set at 120 beats per minute
- Laboratory clamps and clips

Procedure

1. For the first set of experiments, the alkaline cleaner/conditioner bath was prepared according to the manufacturer's specifications by filling the HDPE tank with 24 L of deionized water. Next, 2.88 L of Electro-Brite ML-371 were added, and the tank was brought to a volume of 48 L with deionized water to produce a 6% (by volume) concentration. The solution was gently mixed. For the second set of experiments, the

microetch bath was prepared according to the manufacturer's specifications by filling the HDPE process tank with 24 L of tap water and adding 720 g of copper sulfate pentahydrate ($CuSO_45H_2O$) and 8.64 L of 66° Baume sulfuric acid (H_2SO_4). The acid was added very slowly, taking care that the temperature of the mixture remained below 54° C. A laboratory thermometer was inserted into the mixture to monitor temperature. Next, 3.34 L of Co-Bra Etch Inhibitor Makeup were added, and the mixture was brought to a volume of 48 L with tap water.

2. The stainless steel heating coil was placed into the HDPE tank containing the simulated bath. The coil inlet was connected to tubing from the water bath (with the in-line pump), and the coil outlet connected to tubing discharging back to the water bath. The experimental set up is presented as Figure 7.
3. The Magna-Whirl water bath was filled with approximately 25 gallons of hot tap water. The water bath heater and pump were turned on, allowing the alkaline cleaner and microetch process baths to be heated to 57° C and 52° C, respectively. The water bath thermostat was set, and a thermometer was placed in the bath to constantly monitor its temperature.
4. The bath temperature, pH, and density were measured *in-situ* in the tank Conductivity, viscosity, and surface tension were measured on samples collected from the tank. Analyses were performed as described later in

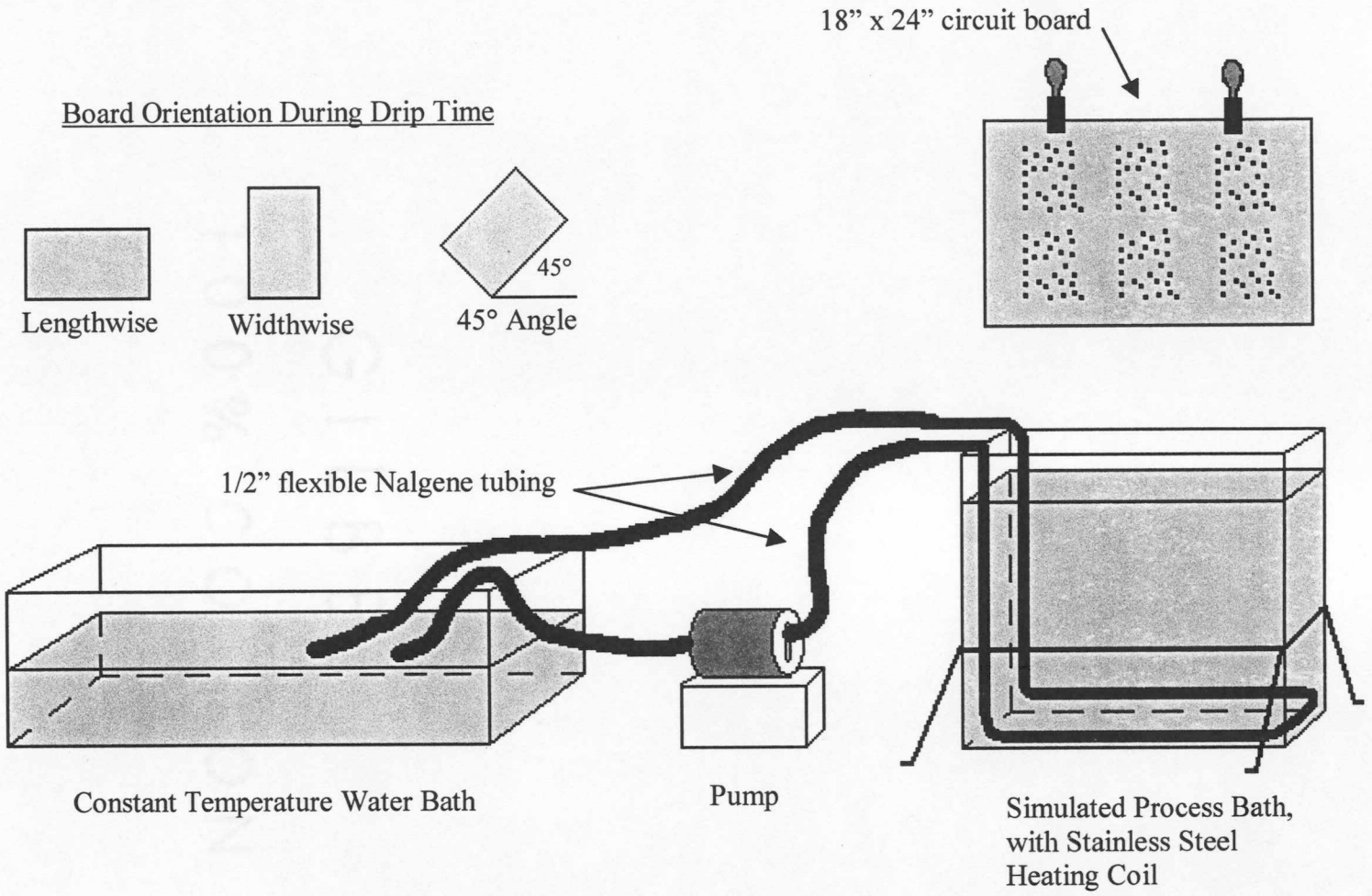

Figure 7. Laboratory Drag-out Experimental Set-Up

the Sample Analyses Section immediately after collection, and the results were recorded.

5. The circuit board was cleaned with tap water and detergent, and thoroughly rinsed with deionized water. The board was dried using compressed air to ensure no moisture remained entrapped in the holes.
6. The board was centered on the analytical balance, and the weight was recorded to the nearest 0.01g.
7. A clean new plastic bag was weighed on the analytical balance, and the results recorded to the nearest 0.01g.
8. The plastic bag was opened, and carefully attached to the outside of the HDPE tank using small laboratory clips.
9. The metronome was turned on, and two laboratory clamps were attached to the circuit board to serve as handles. The circuit board was slowly lowered into the tank so the entire surface was completely submerged in the bath. The board was agitated slightly to remove entrapped air bubbles, and then remained submerged for approximately one minute in the alkaline cleaner/conditioner bath, and 30 seconds in the microetch bath. The process was timed by counting ticks on the metronome.
10. The board was removed vertically at the appropriate withdrawal rate, stopping several inches above the bath surface. The board was then held steady or given one quick shake, and allowed to drip over the bath for the appropriate drain time, either level or at a 45° angle. The appropriate

withdrawal rates, drain positions, and drain times were specified in the experimental matrix. Both the withdrawal rate and drip time were timed by ticks of the metronome.

11. The board was immediately placed into the plastic bag attached to the tank.. Extra care was taken to ensure that any drips after the specified drain period fell into the bag, and that the sharp corners of the board did not puncture the bag.
12. The clamps were removed from the board, along with the clips holding the bag to the tank. The bag was carefully sealed, removing as much air as possible.
13. The sealed bag containing the circuit board and drag-out was centered on the analytical balance and weighed, the results were recorded to the nearest 0.01g.
14. The circuit board was carefully removed from the bag, and the process was repeated, beginning with weighing a clean new plastic bag.
15. After the specified number of runs were completed for each set of conditions, the bath temperature, pH, and density were again measured *in-situ* in the tank. Conductivity, viscosity, and surface tension were measured on samples collected from the tank. Analyses were performed immediately after collecting the sample, and the results were recorded.
16. The drag-out volumes were calculated.

Before the actual drag-out volume experiments were conducted using simulated bath chemicals, a series of four preliminary tests were conducted to validate the proposed methodology and to verify that the drag-out could be measured accurately and precisely. The preliminary tests also served as practice runs, and allowed for any necessary adjustments to the procedure and apparatus. The coefficients of variation for the first two tests were 0.039 and 0.056 for eleven and nine trials, respectively. The coefficients of variation for the third and fourth tests were 0.007 and 0.008, respectively, for series of seven trials each. Since preliminary tests were not designed to cover the full range of operating variables, the following representative variables were selected: (1) ambient temperature tap water was used to simulate bath chemicals, (2) a 12" x 18" drilled etched board was used in the first two preliminary tests, and an 18" x 24" drilled copper clad board was used for the third and fourth tests, and (3) the circuit board was withdrawn at 0.5 fps, given one quick shake after removal, and allowed to drip for 10 seconds.

Quality Assurance and Quality Control

Prior to the experiments, all laboratory equipment was thoroughly cleaned with detergent followed by a thorough rinse with deionized water. The analytical balance used for weighing the boards was allowed to warm up for at least 30 minutes before any measurements were made. The balance was calibrated using calibration weights at the beginning and end of each laboratory session, to ensure the instrument

had not drifted. A large shield was placed around the balance to decrease the effects of drafts while weighing the board.

Prior to mixing the actual baths, 500 mL test baths were prepared per the manufacturers' product information sheets, and laboratory analyses were performed to use as a baseline for comparison. Temperatures were monitored continuously during the drag-out experiments in the baths by suspending a laboratory thermometer in the tank. Before the tests, the timing of the metronome was checked with a laboratory clock to ensure proper timing. The tank was positioned in front of a fume hood for adequate ventilation, and a large strip of tape was affixed to the fume hood shield at a 45° angle from the horizontal to use as a guide during drain periods. Personal protection equipment such as safety goggles, gloves, and aprons were used whenever feasible. All waste material including plastic bags contaminated with the drag-out chemicals and the used bath chemistry was saved for proper disposal. All laboratory experimental information and data were recorded in a laboratory notebook, with carbon copies given to the principal investigators upon test completion.

Sample Collection and Identification

Sample Collection

Samples were collected for analyses from the laboratory drag-out study tanks in the UT laboratory and from actual process baths and rinse tanks during the PWB industry site visits.

For the laboratory drag-out study in the UT laboratory, grab samples were collected for surface tension and viscosity. The samples were collected directly from the experimental tank in a clean beaker, and the analyses were immediately performed.

Samples were collected during the PWB site visits from the microetch, electroless copper, and anti-tarnish process baths and their succeeding rinse tanks in the Making Holes Conductive (MHC) process line. Grab samples were collected using either a plastic measuring cup or a sampling beaker, which consisted of a plastic beaker with a long handle attached. The sampling container was thoroughly rinsed with the sampling fluid prior to sample collection. The grab sample was then immediately transferred from the sampling cup or beaker into a clean 500 mL HPDE sample bottle and capped. Before the sampling event, pre-printed labels were prepared in duplicate, with one label pre-attached to the sample bottle. After the sample was collected, the remaining label was attached to the Sub-Unit Data Collection Log, and the sample description, person taking the sample, time of sample, sample volume, and method of preservation was recorded in ink. All samples were taken in duplicate, with replicates taken for approximately 20 percent of the samples. The sample bottles were sealed with color-coded tamper-proof tape (to identify the sampler and establish chain-of-custody), and placed in plastic lined containers for transport to the UT laboratory.

Sample Identification

Pre-printed labels were prepared in duplicate before the PWB site visits. The following format was used:

$$FUUTTA_c\text{-}I$$

where:

- F is the facility identification number: 1, 2, 3
- UU is the process code: ME = microetch, EC = electroless copper, AT = anti-tarnish
- TT is the tank type: FB = field blank, MW = make-up water, P1 = first process tank, R1 = first rinse tank, R2 = second rinse tank, etc.
- A_c is the analyte code: M = metals, S = surface tension
- I is the identifier code: A = first sample collected in duplicate, B = second sample collected in duplicate, R = replicate sample.

Sample Analyses

Temperature

Temperature was measured *in-situ* in the laboratory drag-out tanks. In the field, temperature was measured on grab samples collected from the process and rinse tanks. Measurements were made immediately after collection.

Apparatus

- Laboratory thermometer, range 0 to 100° C

Procedure

1. The laboratory thermometer was immersed into the laboratory drag-out tank or sample and allowed to stabilize.
2. The temperature reading was recorded on the Sub-Unit Data Collection Log.
3. The process was repeated, and the thermometer was rinsed with deionized water prior to the next test.

pH

The pH was measured *in-situ* in the laboratory drag-out tanks. In the field, pH was measured on grab samples collected from the process and rinse tanks. Measurements were made immediately after collection.

Apparatus

- Orion Digital Portable pH Meter, Model 250A
- Orion Triode™ pH Electrode, Model 91-57BN
- Beakers, for buffer solution

Reagents

- pH buffers for meter calibration: pH 4.01, pH 7.00, and pH 10.01

Procedure for pH Meter Calibration

1. Approximately 50 ml of the appropriate buffers (pH 4.01 and pH 7.00 for acid sub units, or pH 7.00 and pH 10.01 for alkaline sub units) was poured into two beakers.
2. The pH meter was set to the pH mode.
3. The fill hole cover on the electrode was removed, and the electrode was placed into one of the buffers and agitated.
4. "2nd cal" was pressed on the pH meter. When "READY" was displayed, "YES" was pressed.
5. When "P2" was displayed, the electrode was removed, rinsed with deionized water, and placed into the second buffer solution. When a stable pH was displayed, "YES" was pressed. The meter displayed the electrode slope, and automatically advanced to the MEASURE mode.
6. The electrode was rinsed with deionized water, and was ready for testing the sub unit rinse tanks, process baths, or laboratory drag-out tank.

Procedure for pH Measurements

1. After the meter was calibrated, the electrode was placed into the laboratory drag-out tank or sample and agitated slightly.

2. When the pH display was stable, the pH was recorded on the Sub-Unit Data Collection Log.
3. The electrode was rinsed with deionized water, and the process repeated.

The pH meter was calibrated prior to taking measurements for each sub unit. A two-buffer calibration was performed using the 4.01 and 7.00 buffers for the acid sub units, and 7.00 and 10.01 buffers for the alkaline sub units. The first measurement in a sub unit was made in the samples from the last rinse tank, and the measurements progressed up-line, with the last measurement made on the process bath sample.

Conductivity

Conductivity was measured in the UT laboratory on field samples for the process baths and rinse tanks, along with the laboratory drag-out tanks. The samples were analyzed at a controlled temperature of approximately 25° C.

Apparatus

- Orion Conductivity/Temperature Meter, Model 122

Procedure

1. The sample was placed in a water bath and allowed to equilibrate to 25°C.

2. The meter Conductivity/Temperature Selector knob was turned from OFF to CONDUCTIVITY.
3. The conductivity cell was immersed into the sample.
4. The appropriate conductivity range was selected by turning the Conductivity Range Selector knob.
5. The conductivity reading was recorded on the Sub-Unit Data Collection Log.
6. The conductivity cell was rinsed with deionized water prior to the next test.

Prior to the conductivity measurements on the laboratory drag-out and field samples, the meter was tested for accuracy by taking a measurement of a sample of known conductivity.

The conductivity measurements of the rinse tanks were within the meter range of 0.0 to 199.9 mS/cm; however, as anticipated, the values of some of the process baths were higher. Since conductivity is a nearly linear function of total dissolved solids (Snoeyink and Jenkins, 1980), a 1:10 or 1:100 dilution with deionized water was performed on the sample if the initial reading was above the highest range on the meter. The measurement was then taken on the diluted sample, and the meter reading multiplied by the dilution factor.

The conductivity meter automatically compensates the reading for temperature to 25° C for temperatures up to 50° C, except for acids. Since some of the samples were acids heated above 50° C, all conductivity measurements were made on all samples in the UT laboratory, at a controlled temperature of 25° C.

Viscosity

Viscosity was measured on-site from grab samples collected from the rinse tanks, process baths, and laboratory drag-out tanks.

Apparatus

- Gilmont Falling Ball Viscometer, size 1, with stainless steel ball, range 1 to 10 centipoise.
- Stopwatch
- 2000 ml glass beaker
- Laboratory thermometer, °C

Procedure

1. The temperature of the rinse tank or process bath was taken using the laboratory thermometer.
2. A grab sample was collected from the tank using a 2000 ml beaker. The viscometer, stainless steel ball, and thermometer were immediately

submerged into the sample for approximately one minute to allow the laboratory equipment to equilibrate to the liquid temperature.

3. The inside of the viscometer was rinsed with the sample, then slowly filled with rinse or process bath liquid, making sure no air bubbles adhered to the sides of the viscometer.
4. The temperature of the liquid in the beaker was checked and compared with the tank temperature. In general, if the temperature difference was more than approximately 5°C, the beaker was emptied and a new sample collected.
5. The viscometer was held vertical in the center of the 2000 ml beaker. (The beaker still contained the rinse or process liquid, which acted as a temperature bath for the viscometer.) The stainless steel ball was carefully placed by hand into the filled viscometer, making sure no air bubbles stuck to the ball.
6. A stopwatch was used to time the descent of the ball between the fiducial lines on the viscometer. The time was recorded on the Sub-Unit Data Collection Log.
7. The viscometer and beaker were emptied, and the process repeated.
8. Using the mean descent time, the viscosity was calculated as follows:

$$\mu = K(\rho_f - \rho)t \qquad \text{Equation 23}$$

where:

μ = dynamic viscosity, centipoise
K = viscometer constant (0.257 with stainless steel ball, based on laboratory calibration tests using deionized water and sucrose solutions, described below)
ρ_f = density of ball, mg/l (8.02 for stainless steel ball)
ρ = density of liquid, mg/l
t = time of descent, minutes

9. The viscosity was recorded on the Sub-Unit Data Collection Log.
10. The viscometer, stainless steel ball, and beaker were thoroughly rinsed with deionized water prior to the next test.

Before viscosity measurements were made in the field and on the laboratory drag-out tanks, a series of tests were performed to establish the viscometer constant, K, for the falling ball viscometer. The constant was obtained by measuring the time of descent of the stainless steel ball in standard solutions of known viscosity, and was calculated using the following relationship:

$$K = \frac{\mu}{(\rho_f - \rho)t} \qquad \text{Equation 24}$$

Three solutions were used in the investigation: 30 percent sucrose (by weight), 40 percent sucrose (by weight), and deionized water. Before the sucrose solutions were prepared, the sucrose was dried in a desiccator, and all glassware was cleaned and completely air dried. A 1000 ml volumetric flask was weighed on an electronic analytical balance, and the weight recorded to the nearest 0.01 gram. The appropriate amount of sucrose was weighed on the analytical balance (338.10 g and

470.60 g for the 30 percent and 40 percent solutions, respectively), and added to the clean, dry volumetric flask. Approximately 500 ml of deionized water was added to the flask, and the mixture agitated by swirling. Additional deionized water was added slowly, while being swirled, until the sucrose was completely dissolved and the bottom of the meniscus reached the 1000 ml reference line on the volumetric flask. The solution was allowed to rest to allow any entrapped air bubbles to rise. The volumetric flask containing the solution was weighed on the analytical balance, and the temperature was measured with a laboratory thermometer; both measurements were recorded in a laboratory research notebook.

As a quality control check, and to verify the accuracy of hydrometers, the density of the sucrose solutions and the deionized water was calculated and compared with published values. The density of the sucrose solutions and the deionized water was calculated using the following relationship:

$$D = \frac{m_s}{V} \qquad \text{Equation 25}$$

where:

D = density, g/ml
m_s = mass of solution = mass of volumetric flask and solution - mass of volumetric flask, g/L
V = volume of solution, ml

Prior to the experiments to determine the viscometer constant, the sucrose solutions were gently stirred to ensure a homogeneous mixture. A laboratory thermometer was used to measure the temperatures of the sucrose solutions and

deionized water, and the results were recorded in a laboratory research notebook. To find the time of descent for the stainless steel ball, the tests were performed using the same procedure as described above for the rinse tanks, process baths, and laboratory drag-out tests; with one exception. The experiments were done at an ambient temperature of 20-21°C; therefore the temperature bath in the 2000 ml beaker was unnecessary. Instead, the filled viscometer was held vertical in a 50 ml glass cylinder.

Specific Gravity

Specific gravity was measured *in-situ* in the laboratory drag-out tanks. In the field, specific gravity was measured on grab samples collected from the process and rinse tanks. Measurements were made immediately after collection.

Apparatus

- Hydrometer, Fisherbrand, range 0.890 to 1.000
- Hydrometer, Fisherbrand, range 1.000 to 1.600
- 500 ml glass cylinder (optional)

Procedure

1. For measurements taken on samples, the sample was poured into a 500 ml glass cylinder. The appropriate hydrometer was carefully immersed into the drag-out tank or cylinder, making sure it did not touch the sides.

2. After the hydrometer reached a steady level, the specific gravity was read from the scale.
3. The reading was recorded on the Sub-Unit Data Collection Log, and the process was repeated.
4. The hydrometers were thoroughly rinsed with deionized water prior to the next test.

Before the hydrometers were used for measurements for the rinse tanks, process baths and laboratory drag-out tests, the accuracy of the instruments was verified. Hydrometer readings were taken on deionized water and a 40 percent (by weight) sucrose solution. The temperature of the water and sucrose solution was measured with a laboratory thermometer, and the specific gravity measurements were compared with published values.

Surface Tension

Surface tension was measured in the UT laboratory on grab samples collected from the rinse tanks, process baths, and laboratory drag-out tanks.

Apparatus

- Fisher Surface Tensiomat, Model 21, with platinum-iridium ring
- 2 inch diameter glass vessel, approximately 1/2 inch deep
- Laboratory thermometer, °C

- Magna-Whirl water bath

Procedure

1. A water bath was prepared to simulate the temperature of the rinse tank or process bath as measured in the field and recorded on the Sub-Unit Data Collection Log.
2. The rinse tank or process bath sample bottles were placed in the water bath, and allowed to equilibrate to the bath temperature. The water bath and sample temperatures were intermittently monitored using the thermometer. The sample bottles remained in the water bath until used for the surface tension measurement.
3. The clean platinum-iridium ring was placed on the hook on the lever arm of the tensiomat.
4. A clean 2-inch diameter glass vessel was filled with a portion of the sample (transferred immediately from the water bath) and placed on the sample table inside the tensiomat.
5. The sample table was raised until the ring was immersed in the liquid to a depth of approximately 1/8-inch.
6. The torsion arm on the tensiomat was released, and the instrument was adjusted to a zero reading by turning the knob on the right side of the case until the index and its image were in line with the mark on the mirror. Care was taken to ensure the ring remained in the liquid by adjusting the

height of the sample table. The knob on the front of the case beneath the main dial was adjusted until the vernier read zero on the outer scale of the dial.

7. The sample table was lowered until the ring was at the surface of the liquid. At the same time, the knob on the right side of the case was adjusted to keep the index in line with the mark on the mirror. The two simultaneous adjustments were continued until the distended film at the surface of the liquid broke.
8. The reading on the scale at the breaking point (surface tension in dynes per centimeter) was recorded on the Sub-Unit Data Collection Log.
9. The liquid was emptied from the glass vessel, and the process was repeated.
10. Both the platinum-iridium ring and glass vessel were rinsed with deionized water prior to the next test.

Prior to the surface tension tests, the calibration of the tensiomat was checked and the platinum-iridium ring was thoroughly cleaned.

To verify the calibration according to the instrument's instruction manual, the ring was placed on the lever arm and the instrument was adjusted to a zero reading. A 600 mg piece of aluminum foil was placed on the ring, and the knob on the right side of the case was adjusted until the index and its image were in line with the mark

on the mirror. The dial reading was recorded, and compared with the calculated surface tension:

$$S = \frac{Wg}{2l} \qquad \text{Equation 26}$$

where:

S	=	dial reading, or apparent surface tension in dynes/cm
W	=	mass (0.6 grams)
g	=	acceleration of gravity (980 cm/sec^2)
l	=	mean circumference of ring (6.00 cm)

The platinum-iridium ring was cleaned per the manufacturer's instructions: the ring was (1) soaked in concentrated nitric acid for approximately 2 minutes, then rinsed with deionized water, (2) rinsed with acetone, followed by deionized water, and (3) flamed with a Bunsen burner.

Sodium and/or Potassium Analysis

Sodium and potassium analyses were conducted in the UT laboratory on grab samples collected from the process baths and rinse tanks.

Apparatus

- Allied Analytical Systems Atomic Absorption Spectrophotometer, IL Video 12, Serial Number 1857
- Sartorius Analytical Balance, Model AC 120S, UT ID Number 427286
- Miscellaneous volumetric flasks and volumetric pipettes

Reagents

- Sodium calibration standard, Fisher Scientific, 1000 mg/L
- Potassium calibration standard, Fisher Scientific, 1000 mg/L
- Potassium chloride (KCl), Fisher Scientific, certified grade
- Lanthanum chloride ($LaCl\ 6H_2O$), Fisher Scientific, certified grade

Procedure

1. A stock potassium chloride solution was prepared by dissolving 23.84 g. of potassium chloride in 250 ml of deionized water in a volumetric flask. This produced a solution of 50,000 mg/L as K, which was used as an ionization suppressant for the sodium samples. A stock solution of lanthanum chloride was prepared by dissolving 12.72 g. of lanthanum chloride in 100 ml of deionized water in a volumetric flask. This produced a solution of 50,000 mg/L as La, which was used as an ionization suppressant for the potassium samples.
2. Sodium and potassium standards were prepared by diluting the Fisher Scientific calibration standards with deionized water to achieve the desired standards concentrations.
3. The samples were prepared by performing dilutions with deionized water to adjust the anticipated analyte concentrations within the linear range of the instrument. Volumetric pipettes and volumetric flasks were used, and the samples were transferred to new, clean 125 ml HDPE sample

bottles. Samples were acidified with ultrapure nitric acid, and ionization suppressants were added to achieve a concentration of 2000 mg/L as K for the sodium samples, and 1000 mg/L as La for the potassium samples.

4. The appropriate lamp was inserted in the atomic absorption spectrophotometer, and a safety check of all settings was performed. The instrument electronics were turned on and allowed to warm up for approximately 30 minutes.
5. The instrument printer, compressed air, and acetylene were turned on. The pilot was lit, the flame adjusted, and the sampling tube was placed in a fresh beaker of deionized water.
6. The instrument was calibrated with the appropriate sodium or potassium standards. A standard curve was printed, and a linear regression performed to check linearity of the curve. If the R^2 value was below 0.9950, the instrument was re-calibrated with fresh standards.
7. The prepared samples were analyzed, beginning with the rinse samples and progressing up-line to the process tank. Approximately ten analyses were run per sample, each lasting approximately eight seconds. Results were printed and transferred to an Excel spreadsheet.
8. The method of standard additions was performed on process bath samples. The samples were diluted 1:1 with known standards and analyzed in the absorption mode. Generally, 0, 50, 100 and 200 mg/L standards were used for potassium analyses, and 0, 20, 50 and 100 mg/L

standards were used for sodium analyses; however, some variation was necessary to keep the concentrations within the instrument's linear range. A plot of absorption verses concentration of added standards was then prepared, from which the actual concentration in the sample was derived. If necessary, standard additions were performed on the succeeding rinse tanks, as described later in this section.

Before and during the atomic absorption analyses, all laboratory glassware and sample bottles were acid washed in accordance with Standard Methods.

The analyte (sodium or potassium) was chosen for a specific bath based on composition data, as provided by either industry representatives, manufacturers' material safety data sheets, or previous research conducted by the University of Tennessee's Center for Clean Products and Clean Technologies (CCPCT).

Atomic absorption analyses were conducted using the least sensitive wavelengths (330.2 nm for sodium, and 404.4 nm for potassium) whenever possible because of the high concentration of analyte in some of the process baths, together with the wide range of anticipated concentrations between the process baths and rinse tanks. Dilutions were still necessary on many of the samples. Some sodium samples with very low concentrations required the use of the most sensitive wavelength (589.0 nm).

In general, the instrument was calibrated at the beginning of each lab session by using five calibration standards within the linear range of the instrument, including a zero standard. The standards used for the least sensitive wavelength for sodium (330.2 nm) were usually 0, 20, 50, 100, and 150 mg/L; however, these occasionally varied depending on the anticipated concentration of the sample. In all cases, the chosen standards bracketed the sample concentration. Standards used for the most sensitive sodium analyses (589.0 nm wavelength) were generally 0, 0.25 0.50. 0.75, 1.0 and 1.25 mg/L. Calibration standards for the least sensitive wavelength for potassium (404.4 nm) were usually 0, 50, 100, 200 and 600 mg/L. As with the sodium analyses, the chosen standards bracketed the sample potassium concentration. Standards checks were performed during the measurements to ensure the instrument had not drifted. Usually the checks were performed after every four or five measurements, but always after ten measurements.

The samples were prepared for analysis by dilution with deionized water to achieve an anticipated analyte concentration within the linear range of the instrument. The anticipated concentrations were based on previous research conducted by the University of Tennessee's CCPCT. Alkali salts were added to the samples and standards as an ionization suppressant. Potassium chloride was added at a concentration of 2000 mg/L to sodium samples, and lanthanum chloride at a concentration of 1000 mg/L was added to the potassium samples. Process and rinse tank samples, with the exception of samples from the electroless copper lines, were

acidified to pH < 2 in accordance with Standard Methods, using ultrapure concentrated nitric acid, along with the standards. Electroless copper samples were not acidified due to the possibility of the baths containing cyanide.

As an interference check, a standard additions analysis was performed on one sample for each process bath, and compared with analysis results performed without standard additions. Whenever there was a difference greater than 10 percent between the two measurements, a standard addition analysis was performed on the duplicate bath sample, and the standard addition results were used. If standard additions were necessary for the process bath samples, the succeeding rinse tank samples were also checked, and the standard additions measurements used.

Quality Assurance and Quality Control

Prior to the site visit to collect the samples, the 500 ml new HDPE sample bottles were thoroughly cleaned with detergent, triple rinsed with deionized water, and allowed to air dry. Field blanks were used to monitor any contamination from the bottles. The field blanks were pre-labeled and filled with deionized water in the UT laboratory prior to the site visits. During the visit, the bottles were opened for approximately two minutes, then re-sealed.

All laboratory equipment transported to the site was thoroughly cleaned according to Standard Methods prior to leaving the UT laboratory, and was again

thoroughly cleaned between sites. All laboratory equipment, including reagents, deionized water, and cleaning supplies were transported from the UT laboratory. The samples remained in the custody of the sampling team until arrival back to the UT laboratory, where they were placed in a limited access, locked cold room until analyses.

CHAPTER IV

RESULTS AND DISCUSSION

Sample Analyses

A variety of sample analyses were performed for this project. Analyses were done both in the UT laboratory and in the field during sample collection site visits to the PWB manufacturers. Tests were conducted on the simulated process baths used for the laboratory drag-out study, grab samples collected during the site visits, and samples collected and transported back to the UT laboratory. In addition, analyses were performed on various solutions of known compositions and characteristics to calibrate instruments and verify accuracy, procedures, and methodology. Temperature, pH, conductivity, viscosity, and specific gravity were measured both in the UT laboratory and in the field at the PWB sites. Surface tension, sodium, and potassium were measured in the UT laboratory.

Prior to the study, fluid properties believed to most likely affect drag-out volume were specific gravity, viscosity and surface tension. Temperature was checked for all analyses (except sodium and potassium), as it has a significant effect on these properties. Conductivity, sodium, and potassium do not necessarily affect the drag-out volume, but were used as a tracer and check on drag-out volumes carried over from the process baths to the succeeding rinse tanks. Sodium and potassium

analyses were done only on samples from the PWB manufacturing facilities, to be used to verify the prediction model. The pH was monitored as an overall verification of other parameters, QA/QC, and safety.

Laboratory Drag-out Study

Analyses of parameters for the alkaline cleaner/conditioner and microetch simulated baths were performed before the drag-out tests were run, and then after the tests were completed. Results of the tests are presented in Table 9 and Table 10.

As expected, variations were insignificant in the bath parameters for the alkaline cleaner/condition bath comparing values before and after the drag-out tests. There were, however, significant variations in the microetch analyses, as expected. Conductivity, specific gravity, and viscosity all increased; possibly due to the elevated concentrations of copper from the etching effect during the printed wiring

Table 9. Alkaline Cleaner/Conditioner Bath Analyses

Parameter	Before tests	After tests
pH	8 65 (58 deg C)	8 47 (57 deg C)
Conductivity	0 21 mS/cm (35 deg C)	0 234 mS/cm (35 1 deg C)
Specific gravity	0 995 (57 deg C)	0 995 (57 deg C)
Surface tension	34 7 dynes/cm	34 7 dynes/cm
Viscosity	0 85 cp	0 87 cp

Table 10. Microetch Bath Analyses

Parameter	Before tests	After tests
pH	-0 42 (53 deg C)	-0.62 (55 deg C)
Conductivity	1374 mS/cm (22 deg C)	1562 mS/cm (22 deg C)
Specific gravity	1.175 (53 deg. C)	1 205 (52 deg C)
Surface tension	71 0 dynes/cm (53 deg C)	60 dynes/cm (51 deg. C)
Viscosity	1 44 cp (49 deg C)	1 59 cp (50 deg C)

board drag-out tests. It should be noted that the variation in bath parameters during the experiments was assumed linear for both baths. This assumption provided estimates for bath properties that were used in the model development.

Conductivity

Conductivity measurements were performed both in the UT laboratory and at the PWB site visits. The instrument automatically compensates for temperature effects, except when the solutions are acidic. Since many of the PWB baths and rinses were acids, and temperature could have a significant effect on the conductance of these solutions, it was determined that all conductivity measurements should be made at the reference temperature of 25° C. The conductivity measurements

originally made in the field at the PWB sites were re-analyzed on samples in the UT laboratory at a controlled temperature of approximately 25° C. At the beginning of each lab session, the conductivity meter was checked against a solution of known conductance to verify accuracy.

The conductivity measurements of the rinse tanks were within the meter range of 0.0 to 199.9 mS/cm; however, as anticipated, the values of some of the process baths were higher. Since conductivity is almost linear with dissolved solids (Snoeyink and Jenkins, 1980), a 1:10 or 1:100 dilution with deionized water was performed on the sample if the initial reading was above the highest range on the meter. The measurement was then taken on the diluted sample, and the meter reading multiplied by the dilution factor.

Two temperature and conductivity readings were taken on each sample, with the mean values reported. Coefficient of variation of all measurements was less than 0.04. Results of the conductivity analyses are included in the Sodium, Potassium, Conductivity, and Surface Tension Results, as Table 11.

Surface Tension

Surface tension measurements were made in the UT laboratory on samples collected during the site visits and samples from the laboratory drag-out study.

Table 11. Sodium, Potassium, Conductivity and Surface Tension Results

Sample ID	Sodium or Potassium AA Analysis		Sample ID	Conductivity	Surface Tension	
	Analyte	Concentration (ppm)		(mS/cm, 25 deg. C)	(dynes/cm)	Temp (deg. C)
1MEP1M	K	20,380	1MEP1S	304,000	76 2	31
1MER1M	K	77 4	1MER1S	1,935	75 9	19
1MER2M	K	<7 5	1MER2S	213	75 6	19
1ATP1M	K	94	1ATP1S	341	73 2	19
1ATR1M	K	<7 5	1ATR1S	229	76 0	20
1ATR2M	K	<7 5	1ATR2S	223	76 3	20
1ATP1M	Na	2 8	1ATP1S	NA	NA	NA
1ECP1M	Na	67,750	1ECP1S	224,000 *	72 2	47
1ECR1M	Na	242	1ECR1S	1,043	74 4	20
1ECR2M	Na	24 5	1ECR2S	224	76 2	20
1MEMWM	K	<7 5	1MEMWS	NA	NA	NA
1MEMWM	Na	20 12	1MEMWS	NA	NA	NA
1MEFBM	K	<7 5	1MEFBS	1 8	76 2	20
2MEP1M	K	62,300	2MEP1S	477,000	78 0	38
2MER1M	K	98 8	2MER1S	2,170	77 0	12
2ECP1M	Na	63,450	2ECP1S	119,600 *	51 2	42
2ECR1M	Na	128 6	2ECR1S	676	73 2	17
2ATP1M	K	<7 5	2ATP1S	NA	75 0	16
2ATR1M	K	<7 5	2ATR1S	NA	76 3	15
2ATP1M	Na	30 8	2ATP1S	353 *	NA	NA
2ATR1M	Na	34 5	2ATR1S	256	NA	NA
2MEMWM	K	<7 5	2MEMWS	NA	NA	NA
2MEMWM	Na	31 36	2MEMWS	NA	NA	NA
2ECFBM	Na	<0 01	2ECFBS	1 9	76 1	17

Table 11. (continued)

Sample ID	Sodium or Potassium AA Analysis		Sample ID	Conductivity	Surface Tension	
	Analyte	Concentration (ppm)		(mS/cm, 25 deg. C)	(dynes/cm)	Temp (deg. C)
3MEP1M-A	Na	41,550	3MEP1S	168,400	77 6	29
3MER1M-A	Na	173 6	3MER1S-A	3,870	75 9	25
3MER1M-B	Na	242	3MER1S-B	4,520	76 0	25
3MER1M-R	Na	289	3MER1S-R	5,280	75 2	25
3ECP1M	Na	72,950	3ECP1S	261,000	56 2	55
3ECR1M-A	Na	109 3	3ECR1S-A	542	75 0	28
3ECR1M-B	Na	173 5	3ECR1S-B	772	72 5	28
3ECR1M-R	Na	191 7	3ECR1S-R	895	74 6	28
3ECR2M-A	Na	24 3	3ECR2S-A	154	75 5	30
3ECR2M-B	Na	24 4	3ECR2S-B	156 1	75 3	30
3ATP1M	Na	111	3ATP1S	543	72 2	28
3ATR1M-A	Na	19 1	3ATR1S-A	151	73 8	43
3ATR1M-B	Na	19 1	3ATR1S-B	152	73 4	43
3ATR1M-R	Na	23 2	3ATR1S-R	165	73 6	43
3MEMWM	Na	23 1	3MEMWS	NA	NA	NA
3MEMWM	K	<7 5	3MEMWS	NA	NA	NA
3ECFBM	Na	<0 01	3ECFBS	1 8	75 0	30

* Precipitate in sample

Before surface tension measurements were made, the instrument was checked and calibrated per the instrument's instruction manual, as described previously in the Methods Section. The surface tension of deionized water was checked at 20°C to verify accuracy. Seven measurements were made, with a mean value of 74.96 dynes/cm, a standard deviation of 2.03 dynes/cm, and a coefficient of variation of 0.027. This mean value is 4.2 percent higher than the expected value of 72 dynes/cm for the deionized water.

Prior to the measurements, the samples were brought to the recorded temperature of the bath or rinse tanks in the field. Two measurements were taken, with the mean value reported. The coefficient of variation for all measurements on the field samples was less than 0.005. Results of the surface tension measurements are included in the Sodium, Potassium, Conductivity, and Surface Tension Results, as Table 11.

Specific Gravity

Specific gravity was measured in the field on grab samples collected from the process baths and rinse tanks, and in the UT laboratory for the simulated baths used for the laboratory drag-out study. Two hydrometers were used in the experiments, to cover the entire range of specific gravity measurements. Prior to the actual measurements, the accuracy of the instruments was checked by measuring the specific gravity of deionized water and a 40 percent (by weight) sucrose solution.

The density of the deionized water and sucrose solution was first checked by weighing a known volume of solution and then applying the density relationship of mass per unit volume. Results of the verification for deionized water resulted in a value 0.15 percent higher than the expected published value of 1.000 at 20°C, and 0.5 percent less than the published value of 1.176 for the 40 percent sucrose solution at 20° C.

For the actual specific gravity measurements, two readings were taken for each sample. Variability between the measurements recorded in any of the field tests was insignificant at less than 0.1 percent. Results of the specific gravity measurements were used for the viscosity determinations that follow in the Viscosity Section, and are presented along with the viscosity results in Table 12.

Viscosity

Viscosity was measured both in the UT laboratory on the drag-out baths and in the field on grab samples collected from the process baths and rinse tanks.

Two falling ball measurements were performed for each test, and the mean descent time was used in the viscosity calculation. Results from the field sampling analyses are presented in Table 12.

Table 12. Viscosity Field Sampling Results

Ball type Stainless
Ball specific gravity 8 02
Viscometer constant 0 257

Company	Date	Sample ID	Temp. (C)	Time (sec)	Mean Time	Specific Gravity	Mean S.G.	Viscosity (cp)
Number 1	4/8/99	Microetch, process, sample #1	30	37	38 5	1 110	1 110	1 140
		Microetch, process, sample #2	30	40		1 110		
		Microetch, rinse #1, sample #1	20	38	37	1 005	1 005	1 112
		Microetch, rinse #1, sample #2	20	36		1 005		
		Microetch, rinse #2, sample #1	20	40	38	1 005	1 004	1 142
		Microetch, rinse #2, sample #2	20	36		1 003		
Number 1	4/8/99	Electroless Cu, process, sample #1	46	42	41 5	1 170	1 170	1 218
		Electroless Cu, process, sample #2	45	41		1 170		
		Electroless Cu, rinse #1, sample #1	21	34	32 5	1 003	1 003	0 977
		Electroless Cu, rinse #1, sample #2	21	31		1 003		
		Electroless Cu, rinse #2, sample #1	20	37	36 5	1 005	1 005	1 097
		Electroless Cu, rinse #2, sample #2	20	36		1 005		
Number 1	4/8/99	Anti-tarnish, process, sample #1	19	42	39	1 003	1 004	1 172
		Anti-tarnish, process, sample #2	19	36		1 005		
		Anti-tarnish, rinse #1, sample #1	20	37	36 5	1 002	1 002	1 097
		Anti-tarnish, rinse #1, sample #2	20	36		1 002		

Table 12. (continued)

Company	Date	Sample ID	Temp. (C)	Time (sec)	Mean Time	Specific Gravity	Mean S.G.	Viscosity (cp)
Number 1	4/8/99	Anti-tarnish, rinse #2, sample #1	20	35	34	1 002	1 002	1 022
		Anti-tarnish, rinse #2, sample #2	20	33		1 002		
Number 2	4/9/99	Microetch, process, sample #1	37	46	42 5	1 175	1 175	1 246
		Microetch, process, sample #2	37	39		1 175		
		Microetch, rinse #1, sample #1	15	41	39	1 004	1 004	1 172
		Microetch, rinse #1, sample #2	15	37		1 004		
Number 2	4/9/99	Electroless Cu, process, sample #1	38	48	48	1 110	1 110	1 421
		Electroless Cu, process, sample #2	38	48		1 110		
		Electroless Cu, rinse #1, sample #1	20	33	31	1 002	1 002	0 932
		Electroless Cu, rinse #1, sample #2	20	29		1 002		
Number 2	4/9/99	Anti-tarnish, process, sample #1	19	40	40	1 005	1 005	1 202
		Anti-tarnish, process, sample #2	19	40		1 005		
		Anti-tarnish, rinse #1, sample #1	16	36	34 5	1 005	1 005	1 037
		Anti-tarnish, rinse #1, sample #2	17	33		1 005		
Number 3	4/9/99	Microetch, process, sample #1	29	45	45 5	1 145	1 145	1 340
		Microetch, process, sample #2	29	46		1 145		
		Microetch, rinse #1, sample #1	24	37	35 5	1 005	1 005	1 067
		Microetch, rinse #1, sample #2	24	34		1 005		

Table 12. (continued)

Company	Date	Sample ID	Temp. (C)	Time (sec)	Mean Time	Specific Gravity	Mean S.G.	Viscosity (cp)
Number 1	4/8/99	Anti-tarnish, rinse #2, sample #1	20	35	34	1 002	1 002	1 022
		Anti-tarnish, rinse #2, sample #2	20	33		1 002		
Number 2	4/9/99	Microetch, process, sample #1	37	46	42 5	1 175	1 175	1 246
		Microetch, process, sample #2	37	39		1 175		
		Microetch, rinse #1, sample #1	15	41	39	1 004	1 004	1 172
		Microetch, rinse #1, sample #2	15	37		1 004		
Number 2	4/9/99	Electroless Cu, process, sample #1	38	48	48	1 110	1 110	1 421
		Electroless Cu, process, sample #2	38	48		1 110		
		Electroless Cu, rinse #1, sample #1	20	33	31	1 002	1 002	0 932
		Electroless Cu, rinse #1, sample #2	20	29		1 002		
Number 2	4/9/99	Anti-tarnish, process, sample #1	19	40	40	1 005	1 005	1 202
		Anti-tarnish, process, sample #2	19	40		1 005		
		Anti-tarnish, rinse #1, sample #1	16	36	34 5	1 005	1 005	1 037
		Anti-tarnish, rinse #1, sample #2	17	33		1 005		
Number 3	4/9/99	Microetch, process, sample #1	29	45	45 5	1 145	1 145	1 340
		Microetch, process, sample #2	29	46		1 145		
		Microetch, rinse #1, sample #1	24	37	35 5	1 005	1 005	1 067
		Microetch, rinse #1, sample #2	24	34		1 005		

Prior to the actual viscosity measurements, a series of tests were conducted to establish the viscometer constant, K, for the falling ball viscometer. The constant was obtained according to the instrument's instructions by measuring the time of descent of the stainless steel ball in standard solutions of known viscosity, and applying the values to a relationship as described under Viscosity in the Methods Section of this report. Deionized water, tap water, 30 percent sucrose (by weight), and 40 percent sucrose (by weight) solutions were used. Uncalibrated results of the measurements (used to determine the viscometer constant, K), along with the expected viscosity values for the test solutions are presented as Table 13. Robinson, Cox and Ducker (1999) performed a statistical analysis, and the resulting viscometer constant, K, was determined to be 0.257. This value was subsequently used for all calculations for the laboratory and field viscosity determinations.

A sample calculation for viscosity (Equation 21) follows:

$$\mu = K(\rho_f - \rho)t$$

$$= 0.257\left(8\,02\frac{mg}{L} - 1.197\frac{mg}{L}\right)\left(\frac{69s}{60\frac{s}{min}}\right) = 2\,02cp$$

Table 13. Viscosity Measured Values Compared to Expected Values used for the Determination of Viscometer Constant, K

Date	Solution	Temp.(C)	Run #	Time (sec)	Uncalibrated Results	Expected
11/13/98	tapwater (glass ball)	not measured	1	151		
			2	160		
			3	153		
			4	142		
			5	147		
			6	150		
				Mean = 150 5 sec		
				St Dev = 6 02 sec		
				Repro = 4%	1 14 cp	1
11/15/98	tapwater (glass ball)	not measured	1	145		
			2	147		
			3	146		
			4	154		
			5	152		
				Mean = 148 8 sec		
				St Dev = 3 96 sec		
				Repro = 2 7%	1 14 cp	1
11/16/98	tapwater (stainless steel)	not measured	1	31		
			2	35		
			3	35		
			4	35		
			5	35		
				Mean = 34 2 sec		
				St Dev = 1 79 sec		
				Repro = 5 2%	1 20 cp	1
12/15/98	distilled water (glass ball)	20 deg C	1	157		
			2	153		
			3	150		
			4	154		
			5	152		
				Mean = 153 2 sec		
				St Dev = 2 59 sec		
				Repro = 1 7%	1 17 cp	1 002 cp
12/15/98	distilled water (stainless steel)	20 deg C	1	32		
			2	32		
			3	32		
			4	31		
			5	31		
				Mean = 31 6 sec		
				St Dev = 0 55 sec		
				Repro = 1 7%	1 11 cp	1 002 cp
12/15/98	Sucrose (40%)	Results inconclusive due to solution mixing error				
12/16/98	Sucrose (40%)	Results inconclusive due to solution mixing error				

Table 13. (continued)

Date	Solution	Temp (C)	Run #	Time (sec)	Uncalibrated Results	Expected
12/18/98	Sucrose (40%)	Results inconclusive due to solution mixing error				
1/11/99	Sucrose (40%) (Stainless steel)	21 deg C	1	200		
			2	throw out (bubble)		
			3	204		
			4	207		
			5	216		
			6	213		
			7	204		
			8	211		
			9	208		
				Mean = 207 9 sec		
				St Dev = 5 28 sec		
				Repro = 2 54%	7 11 cp	5 97 cp
1/13/99	deionized water (Stainless steel)	21 deg C	1	38		
			2	43		
			3	32		
			4	44		
			5	31		
			6	43		
			7	35		
			8	44		
			9	32		
			10	43		
				Mean = 38 5 sec		
				St Dev = 5 52 sec		
				Repro = 14 3%	1 35 cp	0 9779 cp
1/13/99	Sucrose (40%) (Stainless steel)	21 deg C	1	209		
			2	204		
			3	(air bubble)		
			4	205		
			5	202		
				Mean = 205 sec		
				St Dev = 2 94 sec		
				Repro = 1 4%	7 015 cp	5 97 cp
1/14/99	Sucrose (30%) (Stainless steel)	21 deg C	1	98		
			2	92		
			3	97		
			4	96		
				Mean = 95 75 sec		
				St Dev = 2 63 sec		
				Repro = 2 8%	3 300 cp	3 097 cp
1/18/99	Sucrose (30%) (Stainless steel)	21 deg C	1	101		
			2	94		
			3	98		
			4	94		
			5	99		
			6	94		
				Mean = 96 7 sec		
				St Dev = 3 08 sec		
				Repro = 3 18%	3 333 cp	3 097 cp

Table 13. (continued)

Date	Solution	Temp.(C)	Run #	Time (sec)	Uncalibrated Results	Expected
1/18/99	Sucrose (40%) (Stainless steel)	21 deg C	1 2 3 4 5 6	218 193 193 192 216 192 Mean = 200 67 sec St Dev = 12 68 sec Repro = 6 32%	6 867 cp	5 97 cp

Sodium and Potassium

Sodium and potassium analyses were performed by atomic absorption (AA) in the UT laboratory on samples from the process and rinse baths. Sodium and potassium concentrations from the AA analyses (including conductivity measurements for comparison) are presented in the Sodium, Potassium, Conductivity, and Surface Tension Results as Table 11. The sample identification method follows:

FUUTTA-I

where:

- F is the facility identification number: 1, 2, 3
- UU is the process code: ME = microetch, EC = electroless copper, AT = anti-tarnish
- TT is the tank type: FB = field blank, MW = make-up water, P1 = first process tank, R1 = first rinse tank, R2 = second rinse tank, etc.
- A is the analyte code: M = metals, S = surface tension
- I is the identifier code: A = first sample collected in duplicate, B = second sample collected in duplicate, R = replicate sample.

For example, sample ID *1MEP1M* was collected at the first facility, from the first microetch process tank, and was analyzed for metals.

Complete results of the sodium and potassium analyses are presented as Table 14. It provides an overview of all aspects of the analysis for each individual test, including: (1) the wavelength, (2) the range of standards used for instrument

Table 14. Atomic Absorption Analyses Results

Sample ID	Analyte	Date	Wavelength	Standards Range	Dilution	Standards Curve R^2	Standard Additions?	Number of Runs	Mean Concentration (ppm)
1MEP1M-A	K	6/3/99	404 4	0 - 600 0	1 100	0 9987	No	10	20,070
1MEP1M-A	K	6/4/99	404 4	0 - 200 0	1 100	0 9999	0, 50, 100, 200	10	20,380
1MEP1M-B	K	6/3/99	404 4	0 - 600 0	1 100	0 9987	No	10	19,700
1MER1M-A	K	5/28/99	404 4	0 - 600 0	No	0 9982	No	10	71 5
1MER1M-B	K	5/28/99	404 4	0 - 600 0	No	0 9982	No	10	78 8
1MER1M-R	K	5/28/99	404 4	0 - 600 0	No	0 9982	No	10	82 0
1MER2M-A	K	5/28/99	404 4	0 - 200 0	No	0 9999	No	45	<7 5
1MER2M-B	K	5/28/99	404 4	0 - 200 0	No	0 9999	No	20	<7 5
1MER2M-R	K	5/28/99	404 4	0 - 200 0	No	0 9999	No	10	<7 5
1MEFBM-A	K	5/28/99	404 4	0 - 200 0	No	0 9999	No	10	<7 5
1MEFBM-B	K	5/28/99	404 4	0 - 200 0	No	0 9999	No	10	<7 5
1MEMWM-A	K	5/28/99	404 4	0 - 200 0	No	0 9999	No	10	<7 5
1MEMWM-B	K	5/28/99	404 4	0 - 200 0	No	0 9999	No	10	<7 5
1MEMWM-A	Na	6/1/99	330 2	0 - 50 00	No	0 9996	No	10	20 33
1MEMWM-B	Na	6/1/99	330 2	0 - 50 00	No	0 9996	No	10	19 91
1ECP1M-A	Na	5/29/99	330 2	0 - 100 0	1 1000	0 9992	0, 20, 50, 100	10	67,500
1ECP1M-A	Na	6/1/99	330 2	0 - 150 0	1 1000	0 999	No	10	65,300
1ECP1M-B	Na	5/30/99	330 2	0 - 100 0	1 1000	0 9996	0, 20, 50, 100	10	68,000
1ECP1M-B	Na	6/1/99	330 2	0 - 150 0	1 1000	0 999	No	10	62,700
1ECR1M-A	Na	5/28/99	330 2	0 - 150 0	1 1	0 9996	No	10	281
1ECR1M-B	Na	5/28/99	330 2	0 - 150 0	1 1	0 9996	No	10	192
1ECR2M-A	Na	5/28/99	330 2	0 - 150 0	No	0 9996	No	10	23 4

Table 14. (continued)

Sample ID	Analyte	Date	Wavelength	Standards Range	Dilution	Standards Curve R^2	Standard Additions?	Number of Runs	Mean Concentration (ppm)
1ECR2M-B	Na	5/28/99	330 2	0 - 150 0	No	0 9996	No	10	24 1
1ECR1M-R	Na	5/28/99	330 2	0 - 150 0	1 1	0 9996	No	10	254 3
1ECR2M-R	Na	5/28/99	330 2	0 - 150 0	No	0 9996	No	10	26 1
1ATP1M-A	K	6/3/99	404 4	0 - 600 0	No	0 9987	No	10	90 9
1ATP1M-A	K	6/4/99	404 4	0 - 200 0	No	1	0, 50, 100, 200	10	94 0
1ATP1M-B	K	6/4/99	404 4	0 - 600 0	No	0 9993	No	10	97 4
1ATR1M-A	K	5/28/99	404 4	0 - 600 0	No	0 9982	No	20	<7 5
1ATR1M-B	K	5/28/99	404 4	0 - 600 0	No	0 9982	No	20	<7 5
1ATR2M-A	K	5/28/99	404 4	0 - 200 0	No	0 9999	No	10	<7 5
1ATR2M-B	K	5/28/99	404 4	0 - 200 0	No	0 9999	No	10	<7 5
1ATR1M-R	K	5/28/99	404 4	0 - 600 0	No	0 9982	No	20	<7 5
1ATR2M-R	K	5/28/99	404 4	0 - 200 0	No	0 9999	No	10	<7 5
1ATP1M-A	Na	6/1/99	330 2	0 - 150 0	No	0 999	No	10	2 9
1ATP1M-B	Na	6/1/99	330 2	0 - 150 0	No	0 999	No	10	2 6
2MEP1M-A	K	6/4/99	404 4	0 - 600 0	1 500	0 9987	No	10	62,300
2MEP1M-A	K	6/4/99	404 4	0 - 200 0	1 500	0 9999	0, 50, 100, 200	10	62,300
2MEP1M-B	K	6/4/99	404 4	0 - 600 0	1 500	0 9987	No	10	62,150
2MER1M-A	K	5/28/99	404 4	0 - 600 0	No	0 9982	No	10	99 1
2MER1M-B	K	5/28/99	404 4	0 - 600 0	No	0 9982	No	10	98 3
2MER1M-R	K	5/28/99	404 4	0 - 600 0	No	0 9982	No	10	99 0
2MEMWM-A	K	5/28/99	404 4	0 - 200 0	No	0 9999	No	10	<7 5

Table 14. (continued)

Sample ID	Analyte	Date	Wavelength	Standards Range	Dilution	Standards Curve R^2	Standard Additions?	Number of Runs	Mean Concentration (ppm)
2MEMWM-B	K	5/28/99	404 4	0 - 200 0	No	0 9999	No	10	<7 5
2MEMWM-A	Na	6/1/99	330 2	0 - 50 00	No	0 9996	No	10	31 50
2MEMWM-B	Na	6/1/99	330 2	0 - 50 00	No	0 9996	No	10	31 21
2ECP1M-A	Na	6/1/99	330 2	0 - 150 0	1 1000	0 999	No	10	61,800
2ECP1M-A	Na	5/29/99	330 2	0 - 100 0	1 1000	0 9994	0, 20, 50, 100	10	60,700
2ECP1M-B	Na	6/1/99	330 2	0 - 150 0	1 1000	0 999	No	10	61,700
2ECP1M-B	Na	5/30/99	330 2	0 - 100 0	1 1000	0 9997	0, 20, 50, 100	10	66,200
2ECR1M-A	Na	5/28/99	330 2	0 - 150 0	No	0 9996	No	10	129 7
2ECR1M-B	Na	5/28/99	330 2	0 - 150 0	No	0 9996	No	10	125 4
2ECR1M-R	Na	5/28/99	330 2	0 - 150 0	No	0 9996	No	10	130 6
2ECFBM-A	Na	5/26/99	589 0	0 - 1 000	No	0 9978	No	10	<0 01
2ECFBM-B	Na	5/26/99	589 0	0 - 1 000	No	0 9978	No	10	<0 01
2ATP1M-A	K	6/3/99	404 4	0 - 600 0	No	0 9987	No	10	<7 5
2ATP1M-A	K	6/4/99	404 4	0 - 200 0	No	0 9998	0, 50, 100, 200	10	<7 5
2ATP1M-B	K	6/3/99	404 4	0 - 600 0	No	0 9987	No	10	<7 5
2ATR1M-A	K	5/28/99	404 4	0 - 600 0	No	0 9982	No	30	<7 5
2ATR1M-B	K	5/28/99	404 4	0 - 600 0	No	0 9982	No	40	<7 5
2ATR1M-R	K	5/28/99	404 4	0 - 600 0	No	0 9982	No	40	<7 5
2ATP1M-A	Na	6/3/99	330 2	0 - 150 0	No	0 9997	No	10	32 4
2ATP1M-A	Na	6/3/99	330 2	0 - 100 0	No	0 9974	0, 20, 50, 100	10	30 8
2ATP1M-A	Na	6/1/99	330 2	0 - 150 0	No	0 999	No	10	30 6

Table 14. (continued)

Sample ID	Analyte	Date	Wavelength	Standards Range	Dilution	Standards Curve R^2	Standard Additions?	Number of Runs	Mean Concentration (ppm)
2ATP1M-B	Na	6/1/99	330 2	0 - 150 0	No	0 999	No	10	30 2
2ATR1M-A	Na	6/3/99	589 0	0 - 1 000	1 100	0 9974	No	10	33 0
2ATR1M-B	Na	6/3/99	589 0	0 - 1 000	1 100	0 9974	No	10	36 3
2ATR1M-R	Na	6/3/99	589 0	0 - 1 000	1 100	0 9974	No	10	34 1
3MEP1M-A	Na	6/1/99	330 2	0 - 150 0	1 1000	0 999	No	10	33,400
3MEP1M-A	Na	5/29/99	330 2	0 - 100 0	1 1000	1	0, 20, 50, 100	10	38,900
3MEP1M-B	Na	6/1/99	330 2	0 - 150 0	1 1000	0 999	No	8	33,600
3MEP1M-B	Na	5/30/99	330 2	0 - 100 0	1 1000	0 9975	0, 20, 50, 100	10	44,200
3MER1M-A	Na	5/28/99	330 2	0 - 150 0	No	0 9996	No	10	151 9
3MER1M-A	Na	6/3/99	330 2	0 - 150 0	1 1	0 9997	No	10	166 4
3MER1M-A	Na	6/3/99	330 2	0 - 100 0	1 1	0 9984	0, 20, 50, 100	10	173 6
3MER1M-B	Na	5/28/99	330 2	0 - 150 0	1 1	0 9996	No	10	221 1
3MER1M-B	Na	6/3/99	330 2	0 - 150 0	1 5	0 9997	No	10	241 5
3MER1M-B	Na	6/7/99	330 2	0 - 100 0	1 5	0 9996	0, 20, 50, 100	10	242
3MER1M-R	Na	5/28/99	330 2	0 - 150 0	1 1	0 9996	No	10	270 4
3MER1M-R	Na	6/3/99	330 2	0 - 150 0	1 5	0 9997	No	10	292 0
3MER1M-R	Na	6/3/99	330 2	0 - 100 0	1 5	1	0, 20, 50, 100	10	289
3MEMWM-A	Na	5/28/99	330 2	0 - 150 0	No	0 9992	No	10	22 6
3MEMWM-B	Na	5/28/99	330 2	0 - 150 0	No	0 9992	No	10	23 6
3MEMWM-A	K	6/1/99	404 4	0 - 200 0	No	1	No	10	<7 5
3MEMWM-B	K	6/1/99	404 4	0 - 200 0	No	1	No	10	<7 5

Table 14. (continued)

Sample ID	Analyte	Date	Wavelength	Standards Range	Dilution	Standards Curve R^2	Standard Additions?	Number of Runs	Mean Concentration (ppm)
3ECP1M-A	Na	6/1/99	330 2	0 - 150 0	1 1000	0 999	No	10	67,600
3ECP1M-A	Na	5/29/99	330 2	0 - 100 0	1 1000	0 9979	0, 20, 50, 100	10	74,900
3ECP1M-B	Na	6/1/99	330 2	0 - 150 0	1 1000	0 999	No	10	68,000
3ECP1M-B	Na	5/30/99	330 2	0 - 100 0	1 1000	0 9998	0, 20, 50, 100	10	71,000
3ECR1M-A	Na	5/24/99	330 2	0 - 200 0	No	0 9982	No	10	109 3
3ECR1M-B	Na	5/24/99	330 2	0 - 200 0	No	0 9982	No	10	164 6
3ECR1M-B	Na	6/3/99	330 2	0 - 150 0	1 5	0 9997	No	10	182 5
3ECR1M-B	Na	6/3/99	330 2	0 - 100 0	1 5	0 9988	0, 20, 50, 100	10	173 5
3ECR2M-A	Na	5/28/99	330 2	0 - 150 0	No	0 9992	No	10	24 3
3ECR2M-B	Na	5/28/99	330 2	0 - 150 0	No	0 9992	No	10	24 4
3ECR1M-R	Na	5/24/99	330 2	0 - 200 0	No	0 9982	No	10	191 7
3ECFBM-A	Na	5/26/99	589 0	0 - 1 000	No	0 9978	No	10	<0 01
3ECFBM-B	Na	5/26/99	589 0	0 - 1 000	No	0 9978	No	10	<0 01
3ATP1M-A	Na	6/1/99	330 2	0 - 150 0	No	0 999	No	10	121 2
3ATP1M-A	Na	5/29/99	330 2	0 - 50 0	No	0 9971	0, 20, 50	10	113
3ATP1M-B	Na	6/1/99	330 2	0 - 150 0	No	0 999	No	10	122 1
3ATP1M-B	Na	5/30/99	330 2	0 - 50 0	No	1	0, 20, 50	10	109
3ATR1M-A	Na	5/24/99	330 2	0 - 50 00	No	0 9977	No	15	19 1
3ATR1M-B	Na	5/24/99	330 2	0 - 50 00	No	0 9977	No	20	19 1
3ATR1M-R	Na	5/28/99	330 2	0 - 150 0	No	0 9992	No	10	23 2

calibration, (3) the R^2 value from the linear regression for the calibration curve, (4) the dilution ratio (if necessary), (5) if the method of standard additions was used, (6) the number of runs for each analysis, and (7) the mean concentration.

Table 15 presents the data used to calculate the pooled instrumental relative standard deviation for potassium, determined at 0.77 percent. This was based on eighteen potassium samples with a mean sample concentration of 113.6 mg/L, a pooled instrumental variance of 0.76 mg/L, and a pooled instrumental standard deviation of 0.87 mg/L.

Data used to calculate the pooled instrumental relative standard deviation for sodium is presented as Table 16. Seventy-three analyses were performed on sodium samples, with a mean concentration of 60.6 mg/L. The pooled instrumental variance was 0.94 mg/L, and the pooled instrumental standard deviation was 0.97 mg/L. The pooled instrumental relative standard deviation was calculated at 1.60 percent.

Data used to calculate the reproducibility for duplicate and replicate samples is presented in Table 17. The range of relative standard deviation for potassium tests was from 0.17 percent to 6.95 percent for tests run with no standard additions, with a pooled standard deviation of 3.46 mg/L. There were no duplicate or replicate analyses for potassium using the method of standard additions. Sodium relative standard deviation for tests without standard additions ranged from 0.11 percent to

Table 15. Instrumental Standard Deviation for Potassium (K)

Sample ID	Analyte	Date	Number of Runs	Sample Mean Concentration (ppm)	Standard Deviation	Relative Standard Deviation	Variance
1MEP1M-A	K	6/3/99	10	200 7	2 3	1 1%	5 29
1MEP1M-B	K	6/3/99	10	197 0	1 3	0 7%	1 69
1MER1M-A	K	5/28/99	5	71 3	0 7	1 0%	0 49
1MER1M-A	K	5/28/99	5	71 5	0 5	0 7%	0 25
1MER1M-B	K	5/28/99	5	78 8	0 3	0 4%	0 09
1MER1M-B	K	5/28/99	5	78 7	0 2	0 3%	0 04
1MER1M-R	K	5/28/99	5	82 1	0 3	0 4%	0 09
1MER1M-R	K	5/28/99	5	81 8	0 2	0 2%	0 04
1ATP1M-A	K	6/3/99	10	90 9	0 3	0 3%	0 09
1ATP1M-B	K	6/4/99	10	97 4	0 5	0 5%	0 25
2MEP1M-A	K	6/4/99	10	124 6	0 8	0 6%	0 64
2MEP1M-B	K	6/4/99	10	124 3	0 6	0 5%	0 36
2MER1M-A	K	5/28/99	5	99 0	0 4	0 4%	0 16
2MER1M-A	K	5/28/99	5	99 0	0 2	0 2%	0 04
2MER1M-B	K	5/28/99	5	98 2	0 2	0 2%	0 04
2MER1M-B	K	5/28/99	5	98 3	0 2	0 2%	0 04
2MER1M-R	K	5/28/99	5	99 0	0 3	0 3%	0 09
2MER1M-R	K	5/28/99	5	99 0	0 4	0 4%	0 16

Mean sample concentration (ppm)	**113.6**
Pooled Instrumental Variance (ppm)	**0.76**
Pooled Instrumental Standard Deviation (ppm)	**0.87**
Pooled Instrumental Relative Standard Deviation	**0.77%**

Table 16. Instrumental Standard Deviation for Sodium (Na)

Sample ID	Analyte	Date	Number of Runs	Sample Mean Concentration (ppm)	Standard Deviation	Relative Standard Deviation	Variance
1MEMWM-A	Na	6/1/99	10	20 33	0 68	3 3%	0 46
1MEMWM-B	Na	6/1/99	10	19 91	0 22	1 1%	0 05
1ECP1M-A	Na	6/1/99	10	65 3	0 3	0 5%	0 09
1ECP1M-B	Na	6/1/99	10	62 7	0 2	0 3%	0 04
1ECR1M-A	Na	5/28/99	5	139 5	0 9	0 6%	0 81
1ECR1M-A	Na	5/28/99	5	140 5	0 4	0 3%	0 16
1ECR1M-B	Na	5/28/99	5	96 0	0 3	0 3%	0 09
1ECR1M-B	Na	5/28/99	5	95 6	0 2	0 2%	0 04
1ECR2M-A	Na	5/28/99	5	23 6	0 2	0 8%	0 04
1ECR2M-A	Na	5/28/99	5	23 1	0 4	1 7%	0 16
1ECR2M-B	Na	5/28/99	5	23 9	0 7	2 9%	0 49
1ECR2M-B	Na	5/28/99	5	24 1	0 4	1 7%	0 16
1ECR1M-R	Na	5/28/99	5	126 9	1 8	1 4%	3 24
1ECR1M-R	Na	5/28/99	5	127 3	0 7	0 5%	0 49
1ECR2M-R	Na	5/28/99	5	26 2	0 2	0 8%	0 04
1ECR2M-R	Na	5/28/99	5	25 8	0 4	1 6%	0 16
1ATP1M-A	Na	6/1/99	10	2 9	0 2	6 9%	0 04
1ATP1M-B	Na	6/1/99	10	2 6	0 3	11 5%	0 09
2MEMWM-A	Na	6/1/99	10	31 5	0 16	0 5%	0 03
2MEMWM-B	Na	6/1/99	10	31 21	0 18	0 6%	0 03
2ECP1M-A	Na	6/1/99	10	61 8	0 3	0 5%	0 09

Table 16. (continued)

Sample ID	Analyte	Date	Number of Runs	Sample Mean Concentration (ppm)	Standard Deviation	Relative Standard Deviation	Variance
2ECP1M-B	Na	6/1/99	10	61 7	0 3	0 5%	0 09
2ECR1M-A	Na	5/28/99	5	129 6	0 6	0 5%	0 36
2ECR1M-A	Na	5/28/99	5	129 7	0 5	0 4%	0 25
2ECR1M-B	Na	5/28/99	5	126 8	1 9	1 5%	3 61
2ECR1M-B	Na	5/28/99	5	124 0	5 4	4 4%	29 16
2ECR1M-R	Na	5/28/99	5	130 9	0 4	0 3%	0 16
2ECR1M-R	Na	5/28/99	5	130 2	0 3	0 2%	0 09
2ATP1M-A	Na	6/3/99	10	32 4	0 2	0 6%	0 04
2ATP1M-A	Na	6/1/99	10	30 6	0 3	1 0%	0 09
2ATP1M-B	Na	6/1/99	10	30 2	0 3	1 0%	0 09
2ATR1M-A	Na	6/3/99	10	0 330	0 002	0 6%	0 000004
2ATR1M-B	Na	6/3/99	10	0 363	0 002	0 6%	0 000004
2ATR1M-R	Na	6/3/99	10	0 341	0 002	0 6%	0 000004
3MEP1M-A	Na	6/1/99	10	33 4	0 4	1 2%	0 16
3MEP1M-B	Na	6/1/99	8	33 5	0 3	0 9%	0 09
3MER1M-A	Na	5/28/99	5	151 9	0 3	0 2%	0 09
3MER1M-A	Na	5/28/99	5	151 8	0 6	0 4%	0 36
3MER1M-A	Na	6/3/99	10	83 2	0 6	0 7%	0 36
3MER1M-B	Na	5/28/99	5	111 0	0 9	0 8%	0 81
3MER1M-B	Na	5/28/99	5	110 0	0 3	0 3%	0 09
3MER1M-B	Na	6/3/99	10	48 3	0 6	1 2%	0 36

Table 16. (continued)

Sample ID	Analyte	Date	Number of Runs	Sample Mean Concentration (ppm)	Standard Deviation	Relative Standard Deviation	Variance
3MER1M-R	Na	5/28/99	5	135 3	0 4	0 3%	0 16
3MER1M-R	Na	5/28/99	5	135 0	0 3	0 2%	0 09
3MER1M-R	Na	6/3/99	10	58 4	0 5	0 9%	0 25
3MEMWM-A	Na	5/28/99	5	22 2	0 1	0 5%	0 01
3MEMWM-A	Na	5/28/99	5	22 8	0 9	3 9%	0 81
3MEMWM-B	Na	5/28/99	5	23 7	0 8	3 4%	0 64
3MEMWM-B	Na	5/28/99	5	23 4	0 6	2 6%	0 36
3ECP1M-A	Na	6/1/99	10	67 6	0 3	0 4%	0 09
3ECP1M-B	Na	6/1/99	10	68 0	0 5	0 7%	0 25
3ECR1M-A	Na	5/24/99	5	109 5	1 2	1 1%	1 44
3ECR1M-A	Na	5/24/99	5	109 1	0 8	0 7%	0 64
3ECR1M-B	Na	5/24/99	5	164 1	4 8	2 9%	23 04
3ECR1M-B	Na	5/24/99	5	165 0	1 8	1 1%	3 24
3ECR1M-B	Na	6/3/99	10	36 5	0 6	1 6%	0 36
3ECR2M-A	Na	5/28/99	5	24 1	0 4	1 7%	0 16
3ECR2M-A	Na	5/28/99	5	24 3	0 6	2 5%	0 36
3ECR2M-B	Na	5/28/99	5	23 9	0 8	3 3%	0 64
3ECR2M-B	Na	5/28/99	5	24 9	0 7	2 8%	0 49
3ECR1M-R	Na	5/24/99	5	191 1	1 7	0 9%	2 89
3ECR1M-R	Na	5/24/99	5	192 2	1 5	0 8%	2 25
3ATP1M-A	Na	6/1/99	10	121 2	0 9	0 7%	0 81
3ATP1M-B	Na	6/1/99	10	122 1	0 6	0 5%	0 36

Table 16. (continued)

Sample ID	Analyte	Date	Number of Runs	Sample Mean Concentration (ppm)	Standard Deviation	Relative Standard Deviation	Variance
3ATR1M-A	Na	5/24/99	5	20 9	0 7	3 3%	0 49
3ATR1M-A	Na	5/24/99	5	18 0	0 3	1 7%	0 09
3ATR1M-A	Na	5/24/99	5	18 2	0 4	2 2%	0 16
3ATR1M-B	Na	5/24/99	5	18 5	1 4	7 6%	1 96
3ATR1M-B	Na	5/24/99	5	20 9	0 8	3 8%	0 64
3ATR1M-B	Na	5/24/99	5	16 8	1	6 0%	1 00
3ATR1M-B	Na	5/24/99	5	20 1	1	5 0%	1 00
3ATR1M-R	Na	5/28/99	5	23 4	0 7	3 0%	0 49
3ATR1M-R	Na	5/28/99	5	23 0	0 3	1 3%	0 09
Mean sample concentration (ppm)				**60 6**			
Pooled Instrumental Variance (ppm)				**0 94**			
Pooled Instrumental Standard Deviation (ppm)				**0.97**			
Pooled Instrumental Relative Standard Deviation				**1.60%**			

Table 17. Reproducibility for Duplicate/Replicate Samples

Analyte	Analysis	Duplicate/Replicate Sample ID	Sample Conc	X	s^2	s	Relative Standard Deviation	Range of Relative Standard Deviation	Pooled Standard Deviation (ppm)
K	No standard additions	1MEP1M-A	200 7						
		1MEP1M-B	197	198 85	6 84	2 62	1 32%		
		1MER1M-A	71 5						
		1MER1M-B	78 8						
		1MER1M-R	82	77 43	29	5 4	6 95%		
		1ATP1M-A	90 9						
		1ATP1M-B	97 4	94 15	21 1	4 60	4 88%		
		2MEP1M-A	124 6						
		2MEP1M-B	124 3	124 45	0 0450	0 2121	0 17%		
		2MER1M-A	99 1						
		2MER1M-B	98 3						
		2MER1M-R	99	98 80	0 19	0 44	0 44%	0 17% - 6 95%	3 46
	With standard additions	No duplicates/replicates						Not applicable	Not applicable
Na	No standard additions	1MEMWM-A	20 33						
		1MEMWM-B	19 1	19 72	0 756	0 870	4 41%		
		1ECP1M-A	65 3						
		1ECP1M-B	62 7	64 00	3 38	1 84	2 87%		
		1ECR1M-A	140 5						
		1ECR1M-B	95 8						
		1ECR1M-R	127 1	121 13	526	22 9	18 94%		
		1ECR2M-A	23 4						
		1ECR2M-B	24 1						
		1ECR2M-R	26 1	24 53	1 96	1 40	5 71%		

Table 17. (continued)

Analyte	Analysis	Duplicate/Replicate Sample ID	Sample Conc	X	s^2	s	Relative Standard Deviation	Range of Relative Standard Deviation	Pooled Standard Deviation (ppm)
		1ATP1M-A	2 9						
		1ATP1M-B	2 6	2 75	0 045	0 21	7 71%		
		2MEMWM-A	31 5						
		2MEMWM-B	31 21	31 36	0 042	0 205	0 65%		
		2ECP1M-A	61 8						
		2ECP1M-B	61 7	61 75	0 005	0 071	0 11%		
Na (cont)	No standard additions (continued)	2ECR1M-A	129 7						
		2ECR1M-B	125 4						
		2ECR1M-R	130 6	128 57	7 723	2 779	2 16%		
		2ATP1M-A	32 4						
		2ATP1M-A	30 6						
		2ATP1M-B	30 2	31 07	1 37	1 17	3 77%		
		2ATR1M-A	0 33						
		2ATR1M-B	0 363						
		2ATR1M-R	0 341	0 34	0 00028	0 017	4 88%	0 11% - 18 94%	8 05
	With standard additions	1ECP1M-A	67 5						
		1ECP1M-B	68	67 75	0 13	0 35	0 52%		
		2ECP1M-A	60 7						
		2ECP1M-B	66 2	63 45	15 1	3 89	6 13%	0 52% - 6 13%	2 76

18.94 percent, with a pooled standard deviation of 8.05 mg/L. Sodium analyses performed with standard additions showed a relative standard deviation ranging from 0.52 percent to 6.13%, with a pooled standard deviation of 2.76 mg/L.

And finally, Table 18 presents the analytical method (specifically, the method of standard additions or by comparison of standards curve) used to determine the potassium and sodium concentrations. As an interference check, a standard addition analysis was performed on one sample for each process bath, and compared to the analysis performed without standard additions. Whenever there was a difference greater than 10 percent between the two measurements, standard addition analysis was performed on the duplicate bath sample, and the standard addition results were used. The succeeding rinse tank samples were then checked to determine if standard additions should be used.

Table 18. Analysis Method Used for Potassium and Sodium Analysis

Sample ID	Analyte	Analysis Method		Concentration (ppm)
		Standard Additions	Standards Curve	
1MEP1M	K	X		20,380
1MER1M	K		X	77 4
1MER2M	K		X	<7 5
1ATP1M	K	X		94
1ATR1M	K		X	<7 5
1ATR2M	K		X	<7 5
1ATP1M	Na		X	2 8
1ECP1M	Na	X		67,750
1ECR1M	Na		X	242
1ECR2M	Na		X	24 5

Table 18. (continued)

Sample ID	Analyte	Analysis Method		Concentration (ppm)
		Standard Additions	Standards Curve	
1MEMWM	K		X	<7 5
1MEMWM	Na		X	20 12
1MEFBM	K		X	<7 5
2MEP1M	K	X		62,300
2MER1M	K		X	98 8
2ECP1M	Na	X		63,450
2ECR1M	Na		X	128 6
2ATP1M	K	X		<7 5
2ATR1M	K		X	<7 5
2ATP1M	Na	X		30 8
2ATR1M	Na		X	34 5
2MEMWM	K		X	<7 5
2MEMWM	Na		X	31 36
2ECFBM	Na		X	<0 01
3MEP1M-A	Na	X		38,900
3MEP1M-B	Na	X		44,200
3MER1M-A	Na	X		173 6
3MER1M-B	Na	X		242
3MER1M-R	Na	X		289
3ECP1M-A	Na	X		74,900
3ECP1M-B	Na	X		71,000
3ECR1M-A	Na		X	109 3
3ECR1M-B	Na	X		173 5
3ECR1M-R	Na		X	191 7
3ECR2M-A	Na		X	24 3
3ECR2M-B	Na		X	24 4
3ATP1M-A	Na	X		113
3ATP1M-B	Na	X		109
3ATR1M-A	Na		X	19 1
3ATR1M-B	Na		X	19 1
3ATR1M-R	Na		X	23 2
3MEMWM	Na		X	23 1
3MEMWM	K		X	<7 5
3ECFBM	Na		X	<0 01

Laboratory Drag-out Experiments

Laboratory drag-out experiments were conducted on two simulated process baths to determine the range of expected drag-out volumes under various conditions. Because the alkaline cleaner/conditioner and microetch baths have significantly different chemical compositions and properties, these baths were chosen for the experiments to provide a realistic range of drag-out volumes. Bath properties are presented earlier in the Sample Analysis section of this report, as Tables 9 and 10, for alkaline cleaner/conditioner and microetch baths, respectively. Experimental conditions studied were 1) orientation of the board during the drain time, 2) length of the drain time, 3) board withdrawal rate from the bath, and 4) shaking the board at the beginning of the drain period. The boards were oriented lengthwise, widthwise, or at a 45° angle; drain periods of 10 seconds, 20 seconds, and 30 seconds were studied; withdrawal rates of 0.076 m/s (0.25 fps) and 0.305 m/s (1.0 fps) were tested, and the board was either held steady or shaken at the beginning of the drain period. The basic operating conditions (BOC) for the majority of the tests were: 45° drain angle (with the board oriented lengthwise), 10 second drain time, 0.076 m/s (0.25 fps) withdrawal rate, and no shaking after board withdrawal. Nine sets of experiments were conducted on each bath for a total of eighteen sets of drag-out experiments. Several additional experiments were conducted with the microetch bath for a drilled board with a different hole density and design. With experimental repetitions, eighty-one individual tests were performed.

In general, five repetitions were made for each condition for the alkaline cleaner/conditioner experiments, with the circuit board remaining submersed in the bath for one minute on each test. Since the microetch bath changed both the properties of the circuit board and the chemical composition of the bath by etching copper as the tests progressed, only three repetitions for each condition was performed, and the boards were only allowed to remain submersed for 30 seconds. These conditions were taken into account by assuming that the copper etch rate would remain linear over the duration of the experiments. This assumption was verified by weighing the boards before and after the tests to determine the mass of copper etched from the board. Results of the laboratory drag-out volume experiments are presented as Tables 19 and 20 for the alkaline cleaner/conditioner and microetch baths, respectively.

The drag-out volume for each experimental condition was calculated using the mean drag-out weight from the group of tests for the specific condition. This was generally five runs for the alkaline cleaner/conditioner, and three runs for the microetch. In addition to calculating the mean drag-out weight (in grams), the standard deviation and the coefficient of variation of the measurements were checked for each condition. The coefficient of variation was less than 5 percent for all of the experiments.

Table 19. Drag-out Results for Alkaline Cleaner/Conditioner Bath

Test	Board Type	Dragout (mL/ft^2)	Dragout (mL/m^2)	Coefficient of Variation (%)
1 BOC	drilled, design 2	7.23	77.83	3 2
2 BOC, lengthwise orientation	drilled, design 2	7 03	75.67	1.5
3 BOC, widthwise orientation	drilled, design 2	7 56	81 38	2.1
4 BOC, 20 sec. drip time	drilled, design 2	6.34	68 25	4 0
5 BOC, 30 sec drip time	drilled, design 2	6 00	64.59	4.7
6 BOC, 1 fps withdraw	drilled, design 2	9.17	98.71	1.3
7 BOC, with shake	drilled, design 2	7 23	77.83	3.2
8 BOC	undrilled	3 59	38.64	1.6
9 BOC	drilled, etched, design 2	8.29	89 24	3.8

Note: Design 1, 5619 holes; Design 2, 7824 holes.

Table 20. Drag-out Results for Microetch Bath

Test	Board Type	Dragout (mL/ft^2)	Dragout (mL/m^2)	Coefficient of Variation (%)
10 BOC (2/2/99)	drilled, design 2	10 12	108 93	4 3
BOC (2/13/99)	drilled, design 2	10.02	107.86	2.3
BOC (2/13/99)	drilled, design 1	8.68	93 43	3.8
11 BOC, lengthwise orientation	drilled, design 2	11 24	120 99	0 6
12 BOC, widthwise orientation	drilled, design 2	10.50	113 02	0 6
13 BOC, 20 sec drip time	drilled, design 2	9 12	98 17	1 5
14 BOC, 30 sec. drip time	drilled, design 2	8.77	94 40	0 7
15 BOC, 1 fps withdraw	drilled, design 2	12 37	133.15	1 6
16 BOC, with shake	drilled, design 2	10 40	111.95	2 1
17 BOC	undrilled	6.49	69 86	3.8
18 BOC, etched board	drilled, design 1	10 44	112 38	2.2
	drilled, design 2	11 00	118 41	2 1

Note: Design 1, 5619 holes; Design 2, 7824 holes.

The mean drag-out volume of all experimental conditions for the alkaline cleaner/conditioner was 6.94 mL/ft^2, which is approximately 30% less than the mean drag-out volume of 10.00 mL/ft^2 for the microetch bath. The mean drag-out for all experimental conditions for both baths combined was 8.47 mL/ft^2, and was calculated using only data from the same board hole design so as not to skew the results. It appears that drain time has an affect on drag-out volume, as reflected in the decreasing drag-out volumes as drain time increased. It also appears that the drag-out volume increases as the board withdrawal rate decreases. Board tilt and orientation did not show a significant trend to affect the drag-out volume; however, whether the board was drilled or undrilled did show an effect, with significantly less drag-out on the undrilled boards.

It should be noted that there is a slight discrepancy between the measured drag-out volumes reported in this section and the remainder of the study. The drag-out volumes calculated in the Laboratory Drag-out Experiments Section were not adjusted for temperature in the conversion of specific gravity to density. The hydrometers used in the specific gravity measurements provided results at a standard temperature of 20°C instead of 4°C (where the density of water is 1.00 g/cm^3). Temperature compensation was made in the density calculations before comparisons were performed with published prediction equation results and published drag-out volumes, and before the predictive model was developed. An example of the density calculation follows:

$$\rho, g/cm^3 = (\text{measured S.G.})(\rho_{water\ @\ 20°C}, g/cm^3)$$

$$= (0.995)(0.9982\ g/cm^3)$$

$$= 0.993\ g/cm^3$$

Compensation for temperature resulted in about 0.2 percent decrease in density; thus the slight increase in calculated drag-out volumes hereafter.

Comparison of Experimental Drag-out Volumes with Published Prediction Equations

A comparison of experimental results with drag-out prediction equations from the literature was performed for the alkaline cleaner/conditioner and microetch baths. The following four equations from the literature review were compared, with results presented as Figures 8 and 9 for the alkaline cleaner/conditioner and microetch baths, respectively:

1. $f = 0\ 02\sqrt{v \cdot U_w}$ Equation 3

2. $f = \sqrt{\frac{2v \cdot H \cdot U_w}{9g(H + 4U_w t_{dr})}}$ Equation 4

3. $f = k\left(\frac{U_w \cdot \mu}{\rho \cdot g}\right)^m$ Equation 5

4. $\frac{h}{\sqrt{x}} = \left(\frac{\mu/\rho g}{t_w + t_{dr}}\right)^{\frac{1}{2}}$ Equation 20

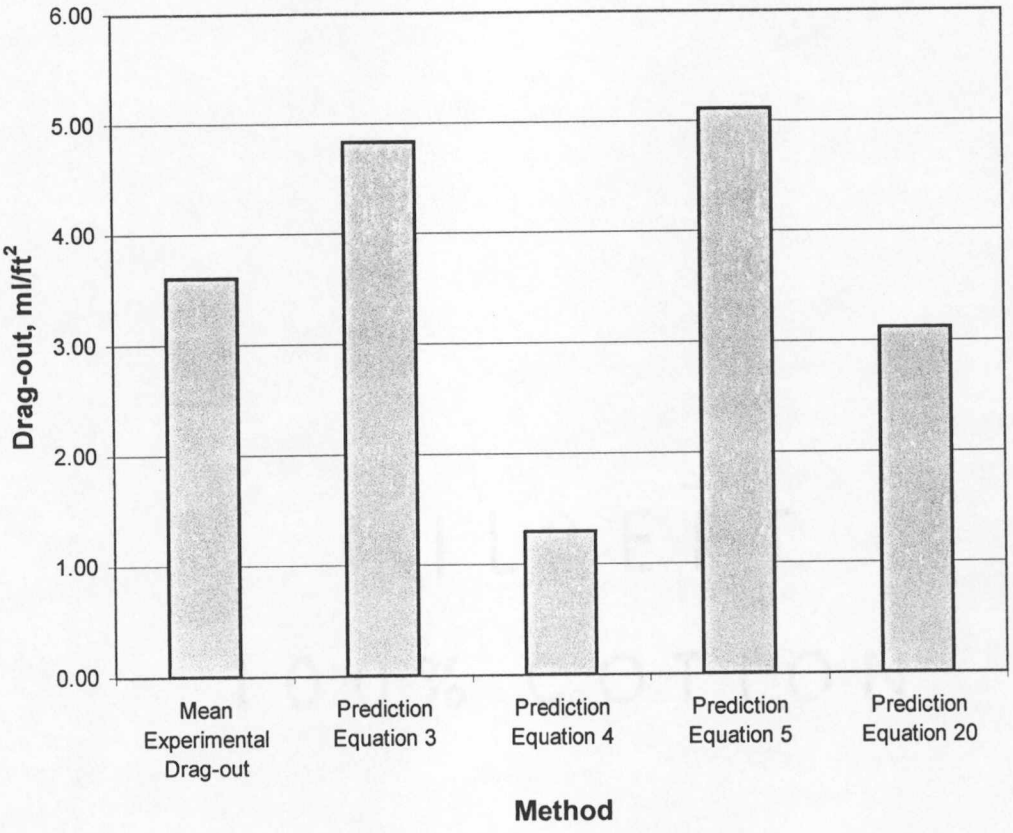

Figure 8. Comparison of Alkaline Cleaner/Conditioner Experimental Drag-out Results with Prediction Equations

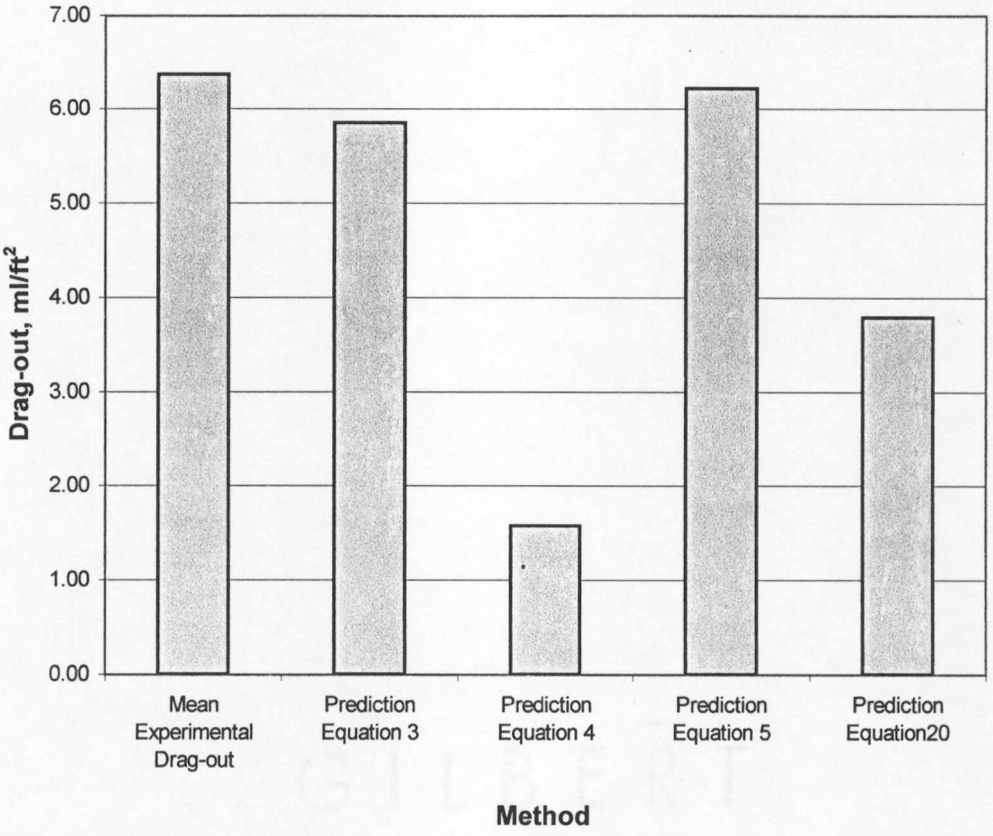

Figure 9. Comparison of Microetch Experimental Drag-out Results with Prediction Equations

A sample calculation for each prediction equation follows:

Equation 3. First, solving for kinematic viscosity,

$$\nu = \frac{\mu}{\rho} = \left(\frac{0.0087 poise}{0.993 \frac{g}{cm^3}}\right)\left(\frac{0.1 \frac{N \cdot s}{m^2}}{poise}\right)\left(\frac{\frac{kg \cdot m}{s^2}}{N}\right)\left(\frac{1000g}{kg}\right)\left(\frac{m}{100cm}\right) = 0.0088 \frac{cm^2}{s}$$

Then, solving for film thickness,

$$f = 0\ 02\sqrt{\nu \cdot U_w}$$

$$= 0.02\sqrt{\left(0.0088 \frac{cm^2}{s}\right)\left(7.6 \frac{cm}{s}\right)} = 0.0052cm$$

And finally, solving for drag-out volume,

$$Dragout = (0.0052cm)\left(\frac{10000cm^2}{m^2}\right)\left(\frac{0.0929m^2}{ft^2}\right)\left(\frac{1ml}{1cm^3}\right) = 4\ 83 \frac{mL}{ft^2}$$

Equation 4. Solving for film thickness,

$$f = \sqrt{\frac{2\nu \cdot H \cdot U_w}{9g(H + 4U_w t_{dr})}}$$

$$= \sqrt{\frac{\left((2)\left(0.0088 \frac{cm^2}{s}\right)(45.72cm)\left(7.6 \frac{cm}{s}\right)\right)}{\left(9\left(981 \frac{cm}{s^2}\right)\left(45.72cm + 4\left(7.6 \frac{cm}{s}\right)(10s)\right)\right)}} = 0.0014cm$$

And solving for drag-out volume using the same method as for Equation 3,

$$Dragout = (0.0014cm)\left(\frac{10000cm^2}{m^2}\right)\left(\frac{0.0929m^2}{ft^2}\right)\left(\frac{1ml}{1cm^3}\right) = 1.3 \frac{mL}{ft^2}$$

Equation 5. As described in the literature review, Equation 5 is an empirical relationship developed by Kushner (1951a), with values for the constants k and *m* derived from the works of others. Kushner recommended a value of k =*2/3,* as proposed by Deryagin, and a value of *m* = *1/2,* as calculated by Kushner from Soderberg's work.

Solving for film thickness,

$$f = k\left(\frac{U_w \cdot \mu}{\rho \cdot g}\right)^m$$

$$= \left(\frac{2}{3}\right)\left(\frac{\left(7.6\frac{cm}{s}\right)(0.0087 poise)\left(\frac{0.1\frac{N \cdot s}{m^2}}{poise}\right)\left(\frac{kg \cdot m}{s^2}\right)\left(\frac{1000g}{kg}\right)\left(\frac{m}{100cm}\right)}{\left(0.993\frac{g}{cm^3}\right)\left(981\frac{cm}{s^2}\right)}\right)^{\frac{1}{2}}$$

$$= 0.0055\ cm$$

And, solving for drag-out volume as above,

$$Dragout = (0\ 0055cm)\left(\frac{10000cm^2}{m^2}\right)\left(\frac{0.0929m^2}{ft^2}\right)\left(\frac{1ml}{1cm^3}\right) = 5.11\frac{mL}{ft^2}$$

Equation 20. The method used to solve Equation 20 is somewhat more complex; specifically numerical integration. The film thickness was calculated using Equation 20 at 1 cm intervals for the *x* coordinate, from zero to 45.72 cm (height of the board

when withdrawn from the bath). The calculated thicknesses were summed, and the total divided by the total number of intervals (47). The resulting value was the mean film thickness used to calculate drag-out volume. An example calculation for film thickness for one interval (25 cm) follows:

$$\frac{h}{\sqrt{x}} = \left(\frac{\mu / \rho g}{t_w + t_{dr}} \right)^{\frac{1}{2}}$$

or, rearranged

$$h = \left(\frac{\mu / \rho g}{t_w + t_{dr}} \right)^{\frac{1}{2}} \cdot \sqrt{x}$$

$$= \left(\frac{(0.0087 poise)\left(0\,1 \frac{N \cdot s}{m^2} \right)\left(\frac{kg \cdot m}{s^2} \right)\left(\frac{1000g}{kg} \right)\left(\frac{m}{100cm} \right)}{\left(0.993 \frac{g}{cm^3} \right)\left(981 \frac{cm}{s^2} \right)} \right)^{\frac{1}{2}} \cdot \sqrt{25cm} = 0.0037cm$$

$$\left(\left(\frac{45\,72cm}{7.6 \frac{cm}{s}} \right) + 10s \right)$$

The mean film thickness for the 47 intervals was calculated at 0.0034 cm. Next, solving for drag-out volume,

$$Dragout = (0.0034cm)\left(\frac{10000cm^2}{m^2} \right)\left(\frac{0.0929m^2}{ft^2} \right)\left(\frac{1ml}{1cm^3} \right) = 3\,12 \frac{mL}{ft^2}$$

Equation 20 predicted drag-out volumes closest to the experimental results for the alkaline cleaner/conditioner bath, predicting volumes approximately 13 percent less than actual test results (3.12 mL/ft^2, versus 3.60 mL/ft^2, respectively). Equations 3 and 5 also predicted volumes reasonably well at about 34 and 42 percent higher (4.83 mL/ft^2 and 5.11 mL/ft^2, respectively). Equation 4 did not perform as well, predicting a drag-out volume about 64 percent less than test results (1.30 mL/ft^2). As mentioned in the literature review, a possible reason for the poor performance of Equation 4 could be that it may only predict drag-out on one side of the board. If this assumption is made, Equation 4 would perform much better, predicting only about 28 percent less than experimental results.

For the microetch bath, Equations 3 and 5 predicted drag-out volumes nearest to the experimental results. Equation 3 predicted a volume approximately 8 percent less than the test results (5.85 mL/ft^2 versus 6.37 mL/ft^2), and Equation 5 predicted about 2 percent below experimental results (at 6.22 mL/ft^2). Equation 20 did not perform as well, predicting around 40 percent less (3.80 mL/ft^2). Again, Equation 4 performed poorly, predicting a drag-out volume about 75 percent less than test results (1.58 mL/ft^2). It should be noted that the above comparisons for the alkaline cleaner/conditioner and microetch baths were made on experiments performed on the undrilled circuit boards, since holes are not accounted for in the published equations.

Comparison of Experimental Results with Published Drag-out Volumes from the Literature

As presented in Table 6 of the literature review, published drag-out volumes vary considerably based on bath type as well as process variables. Reported volumes range from 16 mL/m^2 to 203 mL/m^2. The experimental results for this study resulted in drag-out volumes of 107.6 mL/m^2 for the microetch bath and 74.7 mL/m^2 for the alkaline cleaner bath, resulting in an overall combined experimental drag-out volume of 91.2 mL/m^2 for all tests. These values are well within the published range of drag-out volumes.

A comparison of experimental microetch results with drag-out tests performed at Micom, Inc. (Pagel, 1992) appear somewhat favorable, although a direct comparison is difficult since operating conditions varied. Board hole density for both tests were similar, with Micom boards having 3048 holes/ft^2 versus 2608 holes/ft^2 for this study. Micom's drag-out volumes for a microetch bath appear to be less than the drag-out volumes found in this study; at a withdraw rate of 0.203 m/s (0.667 fps) and drain time of 12.1 seconds, Micom reported a drag-out volume of 7.1 mL/ft^2 (76.4 mL/m^2). Under similar conditions, specifically a withdrawal rate of 0.305 m/s (1.0 fps) and a drain time of 10 seconds, this study resulted in a drag-out of 12.37 mL/ft^2 (133.2 mL/m^2). It should be noted that many other factors could affect the variations in drag-out volumes: (1) for this particular test, a 45° drain angle was used, where Micom used lengthwise board orientation at 0° angle for draining (a 0° drain angle was tested in this study, however, the withdrawal rate was considerably less, at 0.076 m/s), (2) Micom accounted for drag-out volume for racks, and (3) drag-out was

measured by completely different approaches in the two studies; specifically, Micom used a concentration approach where this study used a gravimetric, or weight approach.

Drag-out Prediction Model

The primary objective of this study was to predict the quality of raw wastewater generated from printed wiring board manufacturing; and as discussed previously, one of the main sources of contaminants is from drag-out. From the laboratory study, it is apparent that the literature prediction equations do not consistently provide a dependable drag-out estimate for the wide range of conditions, nor do they account for all of the variables common in the PWB industry. Therefore, a reliable method to predict drag-out was needed.

A statistical analysis was performed on the data from the laboratory drag-out experiments to determine which variables were significant, and to develop a reliable model to predict drag-out volume. The parameters considered for the prediction model are presented in Table 21.

Not all of the parameters listed in Table 21 were chosen as separate variables for the model. For example, the capillary number *(Ca)* was chosen as a variable,

Table 21. Parameters Considered for PWB Drag-out Prediction Model

Bath Fluid Properties	*Process Variables*
pH	Withdrawal Rate
Temperature	Drip Time
Conductivity	Board Hole Density
Viscosity (dynamic and kinematic)	Board Surface (copper or etched)
Density	Board Size
Surface Tension	Board Height
	Drainage Angle
	Shaking after removal

since it is a function of dynamic viscosity, withdrawal rate, and surface tension. Also, since all of the boards used in the laboratory experiments were the same size and the goal was to develop a model for drag-out in units of mL/m^2, board size was not included as a variable. Although board orientation (lengthwise or widthwise) was recorded during the experiments, board height was chosen as a variable instead, as the height could potentially provide more information during the removal stage. (That is, board height combined with withdrawal rate describes the period the board is in an upward motion.) Initially temperature, pH, and conductivity were not believed to be pertinent enough to justify inclusion in the model, since these parameters basically affect other fluid characteristics such as surface tension and

viscosity; however, since the data were available and partially characterizes properties of the bath, it was decided to include them and test their significance.

Board surface type (copper or etched), drainage angle, and board shaking at the beginning of the drainage period were all considered qualitatively by assigning values of 0 or 1 as indicator variables. The indicator variables are listed in Table 22.

Several multiple linear regression models were tested. Backward elimination was used to eliminate any independent variables that did not contribute significantly to the prediction equation. A 10 percent level of significance was used. In addition, one multiplicative regression model with a logarithmic transformation was tested. The goal was to develop a "best fit" prediction equation to the laboratory data, in the simplest form feasible, thus providing a reliable model to predict drag-out.

The first multiple linear regression model form tested follows, and includes all variables (in some form):

Table 22. Indicator Variables for Drag-out Prediction Model

Variable		*Indicator*
Board Surface Type	Copper	0
	Etched	1
Drainage Angle	45°	0
	0°	1
Shake at beginning of drainage period?	no	0
	yes	1

$$DO = a_0 + a_1 pH + a_2 T + a_3 C + a_4 \rho + a_5 Ca + a_6 BH +$$

$$a_7 \angle + a_8 DT + a_9 SH + a_{10} HD + a_{11} BST \qquad \text{Equation 27}$$

where:

DO = Drag-out, mL/m^2
pH = pH
T = Temperature, °C
C = Conductivity, mS/cm
ρ = Bath density, g/cm^3
Ca = Capillary number, ($\mu u_w/\sigma$)
BH = Board height, cm
$\angle$ = Angle, indicator variable
DT = Drip time, sec.
SH = Shake at beginning of drain time, indicator variable
HD = Hole density, number/m^2
BST = Board surface type, indicator variable

The second form of a multiple linear regression model included only terms initially believed to contribute significantly to drag-out. Although this form appears nearly as complex as Equation 27, it contains significantly fewer variables, since the variables are not combined. For example, dynamic viscosity, withdrawal rate, and surface tension are separate independent variables, instead of combined as the capillary number.

$$DO = a_0 + a_1 \rho + a_2 \mu + a_3 \sigma + a_4 WR + a_5 DT + a_6 HD + a_7 \angle + a_8 SH + a_9 BST$$

Equation 28

where:

WR = Withdrawal rate, cm/s

The third model tested includes the same variables as Equation 28, except that the terms for dynamic viscosity, withdrawal rate, and surface tension are combined in the capillary number, and the term for shaking the board at the beginning of the drain time was eliminated:

$$DO = a_0 + a_1\rho + a_2Ca + a_3DT + a_4HD + a_5\angle + a_6BST \qquad \text{Equation 29}$$

And the final multiple linear regression form tested was for comparison with drag-out experiments in the literature; specifically, Micom, Inc. (Pagel, 1992). This form was not expected to perform as well as Equations 27 and 28, since the independent variables were chosen simply because the values were available. It was basically developed to see how well the experimental values from this study correlate with other published values under the same conditions. The final linear form follows:

$$DO = a_0 + a_1HD + a_2WR + a_3DT + a_4\angle \qquad \text{Equation 30}$$

The multiplicative regression model tested was in the following form:

$$DO = a_0 \cdot \rho^{a_1} \cdot Ca^{a_2} \cdot DT^{a_3} \cdot HD^{a_4} \cdot a_5^{angle} \cdot a_6^{BST} \qquad \text{Equation 31}$$

which, after logarithmic transformation, gives the following form that can be analyzed by linear regression:

$$\ln DO = \ln a_0 + a_1 \ln \rho + a_2 \ln Ca + a_3 \ln DT + a_4 \ln HD + \angle \ln a_5 + BST \ln a_6$$

Equation 32

All models were evaluated using JMPIN statistical software (version 3.2), utilizing backwards elimination, and a 10 percent level of significance. Evaluation of Equation 27 resulted in the elimination of pH and board height as variables, as they did not significantly contribute to the prediction equation. For Equation 28, density and shaking were eliminated; and drainage angle was eliminated from Equations 29 and 30. All variables were significant in Equation 32. Table 23 presents the results of the least squares regressions for all models.

Although Equation 27 resulted in the best-fit equation with an R^2 of 0.978, Equation 28 performed almost as good with an R^2 of 0.975, and was chosen as the prediction model since it is a simpler form (only seven primary variables versus eleven). The drag-out prediction model (in the form of Equation 28) follows:

Table 23. Results of R^2 for Prediction Models

Model	R^2
Equation 27	0.978
Equation 28	0.975
Equation 29	0.971
Equation 30	0.439
Equation 32	0.954

$$DO = -0.346 + 2610\,(\mu) + 0.450(\sigma) + 0.982(WR) -$$

$$0.716(DT) + 0\ 00139(HD) + 5\ 28(\angle) + 11.4(BST) \qquad \text{Equation 33}$$

The standard errors, p-values, and 95% confidence intervals for Equation 33 are presented in Table 24.

A comparison of predicted values using Equation 33 verses measured drag-out volumes is presented as Figure 10. It appears from the prediction model (Equation 33), that the drag-out volume is most sensitive to the board hole density, surface tension, and dynamic viscosity, within the expected range of values for these variables. For example, a 10 percent increase in hole density (23,000 holes/m^2 to 25,300 holes/m^2) would result in around 3.2 ml/m^2 more drag-out volume. If surface tension were decreased by 10 percent (by adding a surfactant, for example) from 72

Table 24. Statistics for Drag-out Prediction Model (Equation 33)

Term	*Standard Error*	*p-value*	*Lower 95% Confidence*	*Upper 95% Confidence*
Intercept	2.380	0.8847	-5.08999	4.39721
Dynamic viscosity	670.2	0.0002	1273.06	3944.48
Surface tension	0.1405	0.0020	0.16970	0.72986
Withdrawal rate	0.06671	<0.0001	0.84899	1.11488
Drip time	0.07480	<0.0001	-0.86549	-0.56733
Hole density	0.000058	<0.0001	0.001276	0.001506
Angle	1.172	<0.0001	2.9472	7.6176
Board surface type	1.571	<0.0001	8.31477	14.57868

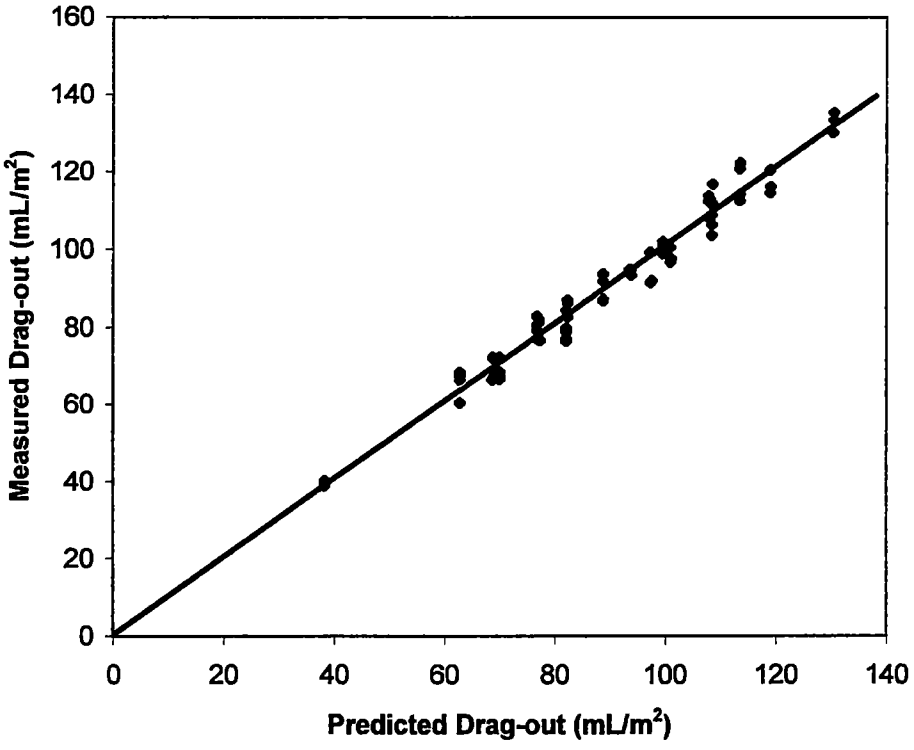

Figure 10. Predicted Drag-out Verses Measured Drag-out

dynes/cm to 66.6 dynes/cm, the drag-out would decrease by about 3.3 ml/m^2. Increasing dynamic viscosity by 10 percent (from 0.0145 poise to 0.0159 poise, which are values similar to a microetch bath), would result in an additional 3.8 ml/m^2. Drag-out volumes for withdrawal rate and drip time varied less than 1 ml/m^2 when the variables were adjusted by 10 percent. Since drainage angle and board surface type are indicator variables, a sensitivity analysis was not applicable.

It should be noted that surface tension was not eliminated from any of the prediction models, indicating that it does have a significant impact (at a 10 percent significance level) on drag-out volume, as initially hypothesized.

And finally, prediction Equation 30 was tested with Micom, Inc. results. The prediction model for Equation 30 follows:

$$DO = 64.2 + 0.00139HD + 0.684WR - 1\ 15DT \qquad \text{Equation 34}$$

Equation 34 predicted a drag-out volume of around 110 mL/m^2 for Micom's data (hole density of 32,809 holes/m^2, withdrawal rate of 20.3 cm/s, and 12.1 second drip time), versus Micom's experimental results of around 76.4 mL/m^2. The predicted drag-out volume is around 44 percent higher than Micom's measured drag-out; however, considering the variations in the test methods, the limited number of variables, and the R^2 of the prediction model, the prediction appears reasonable.

Drag-out Prediction Model Verification

As discussed previously, the primary objective of field sampling and analysis was to validate the drag-out prediction model. In addition to sample collection during the three PWB industry site visits, extensive data were collected that characterized the operating practices for the MHC processes at each site. Summaries

of operating practices and drip times for the field visits were compiled by Robinson, Cox and Ducker (1999), and are presented as Tables 25 and 26, respectively. Again, it should be noted that *ME, EC,* and *AT* represent microetch, electroless copper, and anti-tarnish baths, respectively.

Robinson, Cox and Ducker (1999) developed a dynamic mass balance approach to estimate drag-out volumes at the facilities using the information collected from this study such as field sampling results, process characterizations, operating practices, and other information such as rinsing practices. The same process variables, operating practices, and results from the field sampling analyses were also substituted into the drag-out regression model from this study (Equation 33) to predict drag-out volumes at the PWB facilities.

The drag-out volumes calculated by Robinson, Cox and Ducker (1999) from the field data are presented in Table 27, along with the drag-out volumes from the linear regression prediction model equation (Equation 33) from this study.

Table 25. Summary of MHC Operating Practices for Field Visits (Robinson, Cox and Ducker, 1999)

	Withdrawal rate, m/sec	*Board Tilt, degrees*	*Hole density, number/m^2*
Plant 1	0.173	5	12,500 for ME(A&B) 25,000 for ME(R) 12,500 for EC
Plant 2	0.163	0	NA
Plant 3	0.234	0	50,000

Table 26. Drip Times (Robinson, Cox and Ducker, 1999)

Bath	*Drip time, sec*
Plant 1, ME	5
Plant 1, EC	25
Plant 1, AT	5
Plant 2, ME	10
Plant 2, EC	15
Plant 2, AT	10
Plant 3, ME	5
Plant 3, EC	10
Plant 3, AT	5

Table 27. Drag-out Volumes Calculated from Field Data (Robinson, Cox and Ducker, 1999), and from Prediction Model

Sample Description	*Drag-out from Field Data, mL/m^2 (Robinson, Cox and Ducker, 1999)*	*Drag-out from Prediction Model, mL/m^2 (this study)*
Plant 1, ME	53.6	99.8 (ME-A&B 117 (ME-R)
Plant 1, EC	32.9	85.7
Plant 2, ME	22.8	76.1
Plant 2, EC	23.2	65.0
Plant 3, ME-A	28.2	158
Plant 3, ME-B	41.0	158
Plant 3, ME-R	37.9	158
Plant 3, EC-A	9.73	140
Plant 3, EC-B	6.83	140
Plant 3, EC-R	10.9	140

The drag-out volumes calculated from the prediction model are considerably higher than the drag-out volumes calculated from the field visits. It should be noted that drag-out volumes calculated from the field visits appear unreasonably low, as compared to published values from the literature (Table 6) and from the literature prediction equations. For example, the electroless copper values for plant 3 range from 6.83 to 10.9 mL/m^2, and Pinkerton (1984) suggested that 16 ml/m^2 would be the absolute minimum drag-out on a vertical sheet. The apparent low values from the field drag-out volume estimates could be the result of several factors. The most probable factor is the assumption of instantaneous complete mixing when the boards (and the drag-out) enter the rinse tank. In general, the samples were collected immediately after the boards were placed in the rinse tanks. Therefore, if complete instantaneous mixing occurred, the samples would show the maximum contaminant concentration, and thus allow drag-out prediction. Robinson, Cox and Ducker (1999) hypothesized that short-circuiting most likely occurred in the rinse tanks, producing erroneously low drag-out estimates, due to a significant amount of contaminants potentially lost over the weir of the rinse tank before the samples were collected. It should also be mentioned that Robinson, Cox and Ducker noted that at Plant 3, samples labeled *A* in Table 27 were collected just prior to the boards entering the rinse tank, and theoretically should correspond to the lowest concentrations in the rinse tank. Samples designated as *B* and *R* were taken immediately after the boards were placed in the rinse tanks, and should be close to the maximum concentration in the rinse tanks. It was also noted by Robinson, Cox and Ducker, that samples from

Plant 3, labeled ME-A, ME-B, and ME-R may be falsely low, as they were collected soon after the MHC line had been shut down for a short period of time.

Another potential cause for the prediction model estimating higher values (particularly at Plant 3) could be that the hole density at Plant 3 is considerably higher than the data range used to develop the prediction model; and hole density has a significant impact on drag-out. As previously discussed, the prediction model was developed using linear regression, with the data set containing hole densities of 0 to around 28,100 holes/m^2. The density for the boards at Plant 3 was around 50,000 holes/m^2; therefore, the prediction model is not valid since linear regression predictions are only applicable to the data range used for model development.

Although the drag-out volumes from the prediction model were not validated very well by the field visits, they do compare quite favorably with other works. The study at Micom, Inc. (Pagel, 1992) estimated microetch volumes ranging from around 72 to 130 mL/m^2, or only about 13.7 percent less that the prediction model estimated values, ranging from 76.1 to 158 mL/m^2. A comparison of electroless copper results were not as good, but were still reasonable with Micom's range of 31 to 65 mL/m^2, compared to the prediction model estimates of 65 to 140 mL/m^2, or about double. Overall mean drag-out from the prediction model for the conditions tested in Table 27 was around 106 mL/m^2. This compares generally very well with

the published values from the literature review (Table 6), where values ranged from 16 to 203 mL/m^2.

CHAPTER V

CONCLUSIONS

The manufacture of printed wiring boards is primarily a wet chemistry process with the potential to significantly impact public health and the environment if wastewaters are not properly treated. To ensure adequate treatment, the chemical composition of the wastewater must be determined. This research focused on methods to predict drag-out, which is the main source of contamination in the raw wastewater. With a reliable method to predict drag-out mass, the wastewater quality can be predicted by applying a mass balance to the overall process.

Several predictive equations were identified in the literature that estimate the thickness of the film that adheres to a circuit board as it is withdrawn from the process bath. The most common relationships are basically a function of fluid viscosity and board withdrawal rate, and to a lesser degree surface tension. However, the literature equations do not account for additional variables common in PWB processes, such as the board hole density, drainage angle, drainage time, if the board is shaken at the beginning of the drainage time, and the board surface type.

A series of laboratory drag-out experiments were conducted to test the literature equations, and to determine which fluid properties and process variables

were most important in determining drag-out. The tests were designed to cover a broad range of fluid properties and process variables encountered in industry, using simulated alkaline cleaner/conditioner and microetch baths. Fluid properties studied were pH, conductivity, temperature, viscosity, density, and surface tension. Process variables tested were withdrawal rate, board orientation (lengthwise or widthwise), board tilted during drain period, shaking the board during drain period, hole density, and board surface type.

Results of the drag-out experiments compared very well with published drag-out volumes found in the literature. The mean drag-out volume for all experiments was around 91 mL/m^2, with literature values ranging from 16 to 203 mL/m^2. Two of the studied literature prediction equations performed very well for the microetch bath, predicting drag-out volumes within 8 percent of the measured values. The equations did not predict as well for the alkaline cleaner/conditioner bath. One equation predicted reasonably well at around 13 percent less than the measured values, but the other equations were very inconsistent, predicting values from around 30 to 40 percent above to about 65 percent below the measured values. The results indicate that the literature equations do not accurately and consistently predict drag-out for the range of variables common in PWB manufacturing.

Statistical analyses of the data from the laboratory drag-out experiments were performed to develop a predictive drag-out model relevant to PWB processes.

Several model forms were tested (primarily linear regression with backwards elimination) with the simplest best fit (R^2 = 0.975) equation chosen as a predictive model. Dynamic viscosity, surface tension, withdrawal rate, drip time, hole density, whether the board was tilted during the drip period, and the board surface type were all significant variables (at a 10 percent level of significance). Parameters with the greatest impact on drag-out appear to be hole density, surface tension, and dynamic viscosity. Results of the statistical and sensitivity analyses support the hypothesis that surface tension is an important variable in predicting drag-out.

Several PWB facilities were visited to collect samples and characterize the processes, in an attempt to verify the drag-out prediction model. A dynamic mass balance approach was used (separate from this study) to predict the drag-out from the field visits. The results were somewhat disappointing, as the calculated drag-out volumes from the field visits were much lower than expected, as compared to literature values. It is hypothesized that the low values could be attributed to sampling error, short-circuiting in the rinse tanks, and the erroneous assumption of instantaneous complete mixing.

In conclusion, it appears that surface tension and board hole density are two variables that have a significant impact on drag-out volume in PWB processes. These parameters have not historically been included in theoretical prediction equations found in the literature, which could account for the poor, inconsistent performance.

This research produced an empirical prediction equation with variables relevant to the PWB manufacturing processes.

Recommendations for Future Work

This work resulted in a reliable method to predict drag-out within the range of experimental conditions studied. The simulated alkaline cleaner/conditioner and microetch baths provided a broad range of fluid properties, such as bath density, surface tension, viscosity, and conductivity. The experiments also studied several different process variables, such as withdrawal rate, drip time, and tilting or shaking the board during the drainage period. However, the data were very limited considering the range of potential variables in PWB processes.

Previous work has not studied the effects of board hole density, and the effects of surface tension are limited. Since this research identified these parameters as significant variables in predicting drag-out, more work is warranted to thoroughly quantify their effects. In addition, this study did not consider hole aspect ratios, which could also have a significant effect on drag-out, as drag-out may tend to drain from larger holes and remain entrained in smaller holes. More laboratory drag-out experiments should be conducted to encompass a broader range of board hole densities, fluid surface tension, and the impact of board hole aspect ratios.

REFERENCES

REFERENCES

APHA-AWWA-WPCF, *Standard Methods for the Examination of Water and Wastewater, 17th Ed.*, Washington, D.C., American Public Health Association (1992).

Buczko, Z., "The Modelling of a Rinsing Process in Electroplating Lines," *The Chemical Engineering Journal*, **49**, 161-166 (1992).

Chang, L., and McCoy, B.J., "Waste Minimization for Printed Circuit Board Manufacture," *Hazardous Waste & Hazardous Materials*, **7**, No. 3, 293-318 (1990).

Daugherty, R.L., Franzini, J.B., and Finnemore, E.J., *Fluid Mechanics with Engineering Applications*, 8th Ed., McGraw-Hill, New York (1985).

Denson, C.D., "The Drainage of Newtonian Liquids Entrained on a Vertical Surface," *Ind. Eng. Chem. Fundam.*, **9**, No. 3, 443-448 (1970).

Gutfinger, C. and Tallmadge, J.A., "Films of Non-Newtonian Fluids Adhering to Flat Plates," *A.I.Ch.E. Journal*, **11**, No. 3, 403-412 (May, 1965).

Hanson, N.H., and Zabban. W., "Design and Operation Problems of a Continuous Automatic Plating Waste Treatment Plant," *Plating*, 909-918 (August, 1959).

Kushner, J.B., "Where Do We Go From Here? Part III – Water Control," *Metal Finishing*, **47**, No. 12, 52-58, 67 (1951).

Kushner, J.B., "Dragout Control – Part I," *Metal Finishing*, **49**, November, 59-64 (1951).

Kushner, J.B., "Dragout Control – Part II," *Metal Finishing*, **49**, December, 58-61,67 (1951).

Lang, K.C., and Tallmadge, J.A., "A Postwithdrawal Expression for Drainage on Flat Plates," *Ind Eng. Chem Fundam.*, **10**, No. 4, 648-650 (1971).

Lapin, L.L., *Modern Engineering Statistics*, Duxbury Press, Belmont, CA (1997).

Ledding, A.E., "Estimating Chemical Concentration in Rinse Tanks," *Metal Finishing*, **84**, No. 6, 85-87 (June, 1986).

Lee, C.Y., and Tallmadge, J.A., "Meniscus Shapes in Withdrawal of Flat Sheets from Liquid Baths. II. A Quasi-One-Dimensional Flow Model for Low Capillary Numbers," *Ind. Eng Chem. Fundam.*, **14**, No. 2, 120-126 (1975).

McKesson, D., and Wegener, M.J., "Rinsewater Quality ... Hard Data," *Proceedings of the Technical Conference IPC Printed Circuits Expo '98*, p. S09-1-1 to S09-1-5, The Institute for Interconnecting and Packaging Electronic Circuits, Long Beach, CA (1998).

Mooney, T., "Water Rinsing," *Metal Finishing: 59th Guidebook-Directory Issue 1991*, **89**, No. 1A (January, 1991).

Pagel, P., *Modifications to Reduce Drag-out at a Printed Wiring Board Manufacturer*, EPA/600/R-92/114, Risk Reduction Laboratory, Office of Research and Development, U.S. Environmental Protection Agency, Cincinnati, Ohio (1992).

Pinkerton, H.L., and Graham, A.K., "Rinsing," in *Electroplating Engineering Handbook*, Lawrence J. Durney, Ed., van Nostrand Rheinhold, New York (1984).

Robinson, R.B. and Cox, C.D., *QA/QC Plan for Verification of Hot Solder Finishing: Prediction of Water Quality from Printed Wiring Board Processes*, University of Tennessee, Knoxville, TN (1998).

Robinson, R.B., Cox, C. and Ducker, J., "Prediction of Water Quality from Printed Wiring Board Processes," Final Report to U.S. Environmental Protection Agency and the UT Center for Clean Products and Clean Technologies (August, 1999).

Sharp, J., Teredyne Corp., Nashua, NH., Personal communication with R.B. Robinson (September, 1998).

Snoeyink, V.L., and Jenkins, D., *Water Chemistry*, John Wiley & Sons, New York (1980).

Soroka, A.J., and Tallmadge, J.A., "A Test of the Inertial Theory for Plate Withdrawal," *A.I.Ch E Journal*, **17**, No. 2, 505-508 (1971).

Süβ, Von M., "Technologische Maβnahmen zur Minimierung von Ausschleppverlusten (Technological Measures for Minimizing Drag Out)," *Galvanotechnik*, **81**, No. 11, 3873-3877, (1990).

Süβ, Von M., "Bestimmung Elektrolytspezifischer Ausschleppverluste (Determination of Electrolyte Specific Losses Due to Drag-out)," *Galvanotechnik*, **83**, No. 2, 462-465 (1992).

Tallmadge, J.A., "A Withdrawal Theory for Ellis Model Fluids," *A.I.Ch E Journal*, **12**, No. 5, 1011-1014 (September, 1966).

Tallmadge, J. A. and Gutfinger, C., "Entrainment of Liquid Films, Drainage Withdrawal and Removal," *Ind Eng Chem.*, **59**, No. 11, 19-34 (1967).

Tallmadge, J.A. and Soroka, A.J., "The Additional Parameter in Withdrawal," *Chemical Engineering Science*, **24**, 377-383 (1969).

Tekić, M., and Duduković, A., "A Postwithdrawal Drainage of Newtonian Liquid," *Proceedings of the Third Austrian-Italian-Yugoslav Chemical Engineering Conference,* Graz, Austria, 58-62 (September, 1982).

U. S. Environmental Protection Agency, *Printed Wiring Board Industry and Use Cluster Profile*, Design for the Environment Printed Wiring Board Project (September, 1995).

U.S. Environmental Protection Agency, *Printed Wiring Board Cleaner Technologies Substitutes Assessment Making Holes Conductive*, Vol. 1, Design for the Environment Printed Wiring Board Project, EPA 744-R-98-004A (August, 1998).

White, D.A., and Tallmadge, J.A., "Theory of Drag out of Liquids on Flat Plates," *Chemical Engineering Science*, **20**, 33-37 (1965).

Yost, K.J., "The Computer Analysis of Waste Treatment for a Model of Cadmium Electroplating Facility," *Proceedings Third International Cadmium Conference*, 56-59 (1991).

VITA

Jennie Harper Ducker was born in Jackson County, Ohio on February 20, 1960. She attended public schools in Jackson, Ohio, and graduated from Jackson High School in May, 1978. She attended Ohio Northern University in Ada, Ohio for three years before entering the workforce as a technician for the Crawford County Engineer in Bucyrus, Ohio. After several years, her family moved back to Jackson, where she served as pretreatment coordinator for a municipal wastewater treatment facility. During her time at the WWTP, the pretreatment program was nominated by Ohio EPA for a national pretreatment excellence award. During the same period, she received Class III wastewater and Class I water operator certifications. In 1989, after relocating to Indianapolis, Indiana, Jennie worked for World Wide Chemicals as an environmental compliance coordinator, and for Clean Harbors Environmental Services as an account manager. In 1993, she enrolled at the University of Tennessee in Knoxville, where she received a B.S. (cum laude) in Civil Engineering in May of 1997. After graduation, she worked as an engineer for Harding Lawson Associates in Knoxville, until August, 1998, when she returned to the University of Tennessee to pursue a Master of Science degree in Environmental Engineering. She received her master's degree in May, 2000.

Jennie currently resides near Denver, Colorado, where she plans to work in the industrial sector.